

## Drawing Halin-graphs with small height

Therese Biedl<sup>1</sup> Milap Sheth<sup>1</sup>

<sup>1</sup>David R. Cheriton School of Computer Science,  
University of Waterloo, Waterloo, Ontario N2L 1A2, Canada.

Submitted: November 2021

Reviewed: April 2022

Revised: July 2022

Accepted: August 2022

Final: September 2022

Published: September 2022

Article type: Regular paper

Communicated by: S. Kobourov

**Abstract.** In this paper, we study how to draw Halin-graphs, i.e., planar graphs that consist of a tree  $T$  and a cycle among the leaves of that tree. Based on tree-drawing algorithms and the pathwidth  $pw(T)$ , a well-known graph parameter, we find poly-line drawings of height at most  $6pw(T) + 3 \in O(\log n)$ . We also give an algorithm for straight-line drawings, and achieve height at most  $12pw(T) - 1$  for Halin-graphs, and smaller if the Halin-graph is cubic. We show that the height achieved by our algorithms is optimal in the worst case (i.e. for some Halin-graphs).

## 1 Introduction

It is well-known that every planar graph has a planar straight-line drawing in an  $O(n) \times O(n)$ -grid [10, 25] and that an  $\Omega(n) \times \Omega(n)$ -grid is required for some planar graphs [9] (definitions will be given in the following section). But for some subclasses of planar graphs, planar straight-line drawings of smaller area can be found. In particular, for any tree one can easily create a straight-line drawing of area  $O(n \log n)$  [7]; the area can be improved to  $n2^{O(\sqrt{\log \log n \log \log \log n})}$  [6] and  $O(n)$  if the maximum degree is  $O(n^{1-\epsilon})$  [20]. Outer-planar graphs can be drawn with area  $O(n^{1+\epsilon})$  [19] and with area  $O(n \log n)$  if the maximum degree is constant [18] or a constant number of bends are allowed in edges [2]. There are also some sub-quadratic area results for series-parallel graphs [2], though they require bends in the edges.

These existing results suggest that bounding the so-called *treewidth* of a graph may be helpful for obtaining better area bounds. In particular, trees have treewidth 1, and outer-planar and series-parallel graphs have treewidth 2. However, one can observe that the lower-bound graph from [9] can be modified to have treewidth 3, so we cannot hope to achieve sub-quadratic area for

---

Research of TB supported by NSERC.

---

E-mail addresses: [biedl@uwaterloo.ca](mailto:biedl@uwaterloo.ca) (Therese Biedl) [m2sheth@uwaterloo.ca](mailto:m2sheth@uwaterloo.ca) (Milap Sheth)



This work is licensed under the terms of the [CC-BY](https://creativecommons.org/licenses/by/4.0/) license.

all planar graphs of constant treewidth. On the other hand, there are some subclasses of planar graphs that have treewidth 3 and a special structure that may make them amenable to be drawn with smaller area. This is the topic of the current paper.

Halin-graphs were originally introduced by Halin [22] during his study of graphs that are planar and 3-connected and minimal with this property. He showed that any such graph consists of a tree without vertices of degree 2 where a cycle has been added among the leaves of the tree. These graphs have attracted further interest in the literature, see for example [13, 16, 17, 26, 28]. It is folklore that they can be recognized in linear time since they are planar graphs and have treewidth 3, but a direct and simpler approach for this was given by Eppstein [13].

In this paper, we study how to create planar drawings with small area of a Halin-graph. To our knowledge, no such algorithms have been given before, and the best previous result is to apply a general-purpose planar graph drawing algorithm that achieves area  $O(n^2)$ . In contrast to this, we exploit here that a Halin-graph consists of a tree  $T$  with a cycle  $C$  among its leaves, and give two results. The first one states that, given a plane drawing  $\Gamma$  of  $T$ , we can obtain a planar drawing  $\Gamma_C$  of  $T \cup C$  such that the height of  $\Gamma_C$  is at most three times the height of  $\Gamma$ . However,  $\Gamma_C$  has bends. For our second result, we take inspiration from one particular tree-drawing algorithm by Garg and Rusu [21] to create an algorithm that achieves straight-line drawings of area  $O(n \log n)$ . In fact, the height of our drawings, which is  $O(\log n)$  in the worst case, can be bounded more tightly by  $O(pw(T))$ , where the *pathwidth*  $pw(T)$  is a well-known graph parameter. It is known that the pathwidth is a lower bound on the height of any planar graph drawing [15]. Therefore our algorithm gives an  $O(1)$ -approximation algorithm on the height of plane drawings of Halin-graphs. Similarly as was done for trees [27], and ordered trees [1], we can also argue that our bounds are best-possible for some Halin-graphs.

Our paper is structured as follows. After reviewing the necessary background in Section 2, we briefly argue in Section 3 how to use any tree-drawing algorithm to create (poly-line) drawings of Halin-graphs. Section 4 gives the algorithm for straight-line drawings of small height, while Section 5 defines a class of Halin-graphs that have small pathwidth, yet require a large height in any (straight-line or poly-line) planar drawing. We conclude in Section 6.

## 2 Background and notations

We assume familiarity with graphs and basic graph-theoretic terms, see for example [11]. Throughout this paper, we use  $n$  for the number of vertices in a given graph  $G = (V, E)$ . A *tree* is a connected graph without cycles. A *ccw order* at vertex  $v$  is a cyclic order of the incident edges of  $v$ . (The name was chosen since in drawings the edges at  $v$  should appear in this order when enumerated counter-clockwise around  $v$ .) Equivalently, the ccw order also describes a cyclic order of the neighbours. We assume throughout that trees are *ordered*, i.e., come with a ccw order at each vertex. A *leaf* of a tree is a vertex of degree 1. The *cyclic order of the leaves* is the order in which leaves are visited during a traversal that follows edges at each vertex in ccw order.

A *rooted tree* is a tree together with one specified vertex (the *root*); this defines for any edge of the tree a parent-child relationship with the *parent* being the endpoint that is closer to the root. A *rooted path* is a rooted tree where every vertex has at most one child; a single vertex is considered a rooted path. A *binary tree* is a rooted tree where every vertex has at most two children. For any vertex  $v$  in a rooted tree  $T$ , we use  $T_v$  to denote the *subtree of  $T$  rooted at  $v$* , i.e., vertex  $v$  and all its descendants.

In a rooted tree, the term *leaf* is used only for those vertices that have no children, i.e., the root is not considered a leaf unless the tree is a singleton vertex. If a vertex  $v$  is neither leaf nor root,

then the *first* (or *oldest*) child of  $v$  is the child that comes after the parent in the ccw order at  $v$ .<sup>1</sup> At the root, we assume that the first child is explicitly specified. For any vertex  $v$ , the *age-order* of its children is the enumeration according to the ccw order at  $v$  starting with the first child and ending with the *last* (or *youngest*) child. The *age-order of the leaves* is the order in which we visit leaves during a traversal where children are visited in age-order; the first and last element of this order are the *first* and *last* leaf of  $T$ .

**Halin-graphs and skirted graphs:** Let  $T$  be an (unrooted, ordered) tree without vertices of degree 2. To avoid trivialities, we assume that  $T$  has at least three leaves. Let  $H$  be the graph obtained by adding edges to create a cycle among the leaves of  $T$  in cyclic order; this is the *Halin-graph* formed by  $T$  (and sometimes denoted  $H(T)$ ). Tree  $T$  is called the *skeleton* of Halin-graph  $H$ , and the edges of the cycle are called *cycle-edges*. See Figure 1.

Observe that any Halin-graph is *planar*, i.e., can be drawn without crossing in the plane. The condition ‘no vertex has degree 2’ is not crucial for our drawing algorithm (though it was crucial in the original study of Halin-graphs as minimal 3-connected planar graphs [22]). As in [16], we use the term *extended Halin-graph* for a graph  $H(T)$  obtained by taking an arbitrary tree  $T$  and connecting its leaves in cyclic order, while a *regular Halin-graph* refers to a Halin-graph as above, i.e., the skeleton has no vertices of degree 2.

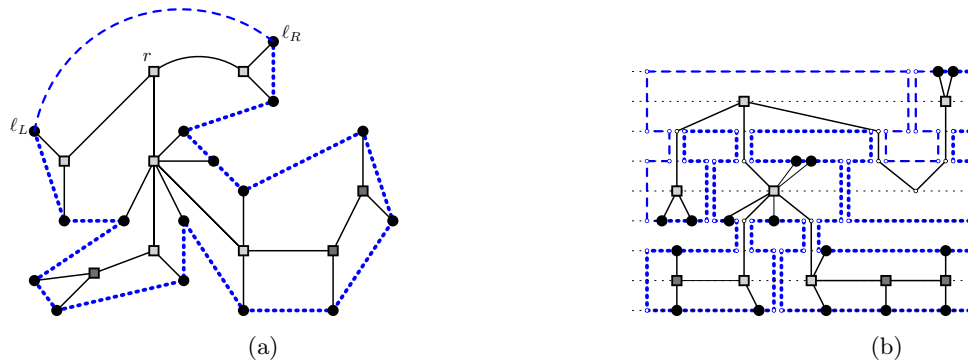


Figure 1: (a) A regular Halin-graph. Cycle-edges are thick blue dotted (or occasionally dashed) throughout the paper. Nodes of skeleton  $T$  are black/gray, and the skirted graph  $H^-(T)$  would omit the dashed cycle-edge if  $T$  were rooted at  $r$ . The inner skeleton uses squares, its leaf-reduction is light gray. (b) A poly-line drawing obtained with the transformation in Section 3.

Our drawing algorithms will be based on rooted, rather than unrooted, trees, and therefore exploit subgraphs of Halin-graphs formed by rooted trees. Let  $T$  be an (ordered) tree that has been rooted at vertex  $r$ . Let  $H$  be the graph obtained by connecting the leaves of  $T$  in age-order in a path; this is the *skirted graph* [26] formed by  $T$  (and sometimes denoted  $H^-(T)$ ). Graph  $H^-(T)$  is a subgraph of  $H(T)$ ; it is missing either an edge  $(\ell_F, \ell_L)$  between the first and last leaf, or (if the root  $r$  has degree 1) the path  $(\ell_F, r, \ell_L)$ .

**Pathwidth and rooted pathwidth:** A *path decomposition* of a graph  $G$  is an ordered sequence  $X_1, \dots, X_\xi$  of vertex-sets (*bags*) such that any vertex belongs to a non-empty subsequence of bags,

<sup>1</sup>The terms *leftmost* is more common than *first/oldest* for children and leaves, but in this paper we reserve “left” for comparing  $x$ -coordinates in a drawing.

and for any edge at least one bag contains both endpoints. The *width* of such a path decomposition is  $\max_i\{|X_i| - 1\}$ , and the *pathwidth*  $pw(G)$  is the minimum width over all path decompositions of  $G$ . A graph consisting of a singleton vertex hence has pathwidth 0.

We will in this paper almost only be concerned with the pathwidth of trees where an equivalent definition is known. For a path  $P$  in a tree  $T$ , let  $\mathcal{T}(T, P)$  denote the connected components of the graph obtained by removing the vertices of  $P$ . Suderman [27] showed that for any tree  $T$  we have

$$pw(T) := \begin{cases} 0 & \text{if } T \text{ is a single vertex,} \\ \min_P \max_{T' \in \mathcal{T}(T, P)} \{1 + pw(T')\} & \text{otherwise,} \end{cases}$$

where the minimum is taken over all paths  $P$  in  $T$ . A path  $P$  that can be used to obtain the minimum for  $pw(T)$  is called a *main path*; it is not unique.

Our constructions will use a rooted tree  $T$ , and therefore employ width-parameters for rooted trees explored in [5] and illustrated in Figure 2. Define the *rooted pathwidth*  $rpw(T)$  to be

$$rpw(T) := \begin{cases} 1 & \text{if } T \text{ is a rooted path,} \\ \min_{P_r} \max_{T' \in \mathcal{T}(T, P_r)} \{1 + rpw(T')\} & \text{otherwise,} \end{cases}$$

where the minimum is over all rooted paths  $P_r$  of  $T$ . (The recursive formula differs from the one for pathwidth only in that the path must end at the root; hence the name.) A path  $P_r$  that can be used to obtain the minimum for  $rpw(T)$  is called a *spine*; it is not unique. Whenever a spine has been fixed, and  $v$  is a node on the spine with a *spine-child* (i.e., a child on the spine), then the remaining children of  $v$  are called *non-spine children* and sometimes distinguished as *before-spine* and *after-spine* children according to age-order. One can show that for any non-spine child  $c$  the subtree  $T_c$  rooted at  $c$  satisfies  $rpw(T_c) < rpw(T)$  [5]. The same paper also shows that for any tree  $T$  and any choice of root of  $T$ , we have  $pw(T) \leq rpw(T) \leq 2pw(T) + 1$ .

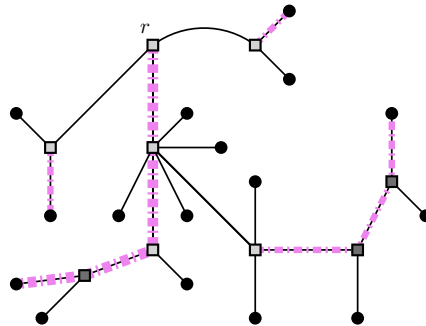


Figure 2: Skeleton  $T$  of the Halin-graph of Figure 1 has  $rpw(T) = 3$  if rooted at  $r$ . Spine-edges are purple (dash-dotted) and thick for a spine  $P_r$  of  $T$ ; thin purple edges are spines of the subtrees that would result from removing  $P_r$ .

**Graph drawing:** A *poly-line* is a simple curve that is the union of finitely many line segments; the transition between two such segments is called a *bend*. A *planar poly-line drawing*  $\Gamma$  of a graph  $G$  consists of assigning a point to each vertex and a poly-line (between the endpoints) to each edge such that all points and poly-lines are disjoint except at incidences of the corresponding graph objects. The drawing is called *straight-line* if there are no bends.

A *flat visibility representation* of  $G$  consists of assigning a horizontal segment  $s(v)$  to every vertex and a horizontal or vertical segment to every edge such that the segment of edge  $(u, v)$  ends at the segments of  $u$  and  $v$ , and segments are disjoint otherwise. In our figures, vertex-segments are thickened into boxes for ease of reading, see e.g. Figure 3.

We assume throughout that identifying features (i.e., points, bends, endpoints of segments) have integral  $y$ -coordinates. The *layers* of a drawing  $\Gamma$  are the horizontal lines with integral  $y$ -coordinate that intersect  $\Gamma$ ; we usually enumerate them from top to bottom as  $1, 2, \dots, h$ . The number  $h$  of layers is called the *height* of  $\Gamma$ . Minimizing the height of drawings is the main objective in this paper. Sometimes we demand integral  $x$ -coordinates as well; we then use the term *column* for a vertical line of integral  $x$ -coordinate that intersects the drawing and let the *width* be the number of columns.

We usually identify the graph object (vertex, edge) with the geometric object (point, poly-line, segment) that it corresponds to in the drawing. Any drawing  $\Gamma$  is required to be *planar* (i.e., without crossing edges) by definition. We often require  $\Gamma$  to be *plane*, i.e. the counter-clockwise cyclic order in which edges are incident to a vertex  $v$  in  $\Gamma$  reflects the ccw order at  $v$  in the ordered tree. For a Halin-graph, a *plane* drawing  $\Gamma$  must also *reflect the outer-face*, i.e., the infinite region of  $\mathbb{R}^2 \setminus \Gamma$  is adjacent to the cycle-edges.

For any drawing where all segments are horizontal or vertical, we can *insert a layer* below layer  $\ell$  by moving all defining features in layer  $\ell' > \ell$  to layer  $\ell' + 1$ ; this maintains a plane drawing and increases the height by 1. Similarly we can insert a column.

### 3 Transforming tree drawings

In this section, we show that any algorithm that gives plane tree-drawings can be used to obtain plane poly-line drawings of Halin-graphs. Our idea is to draw the skeleton-tree  $T$  and insert the cycle-edges  $C$ . As it will turn out, it suffices to take a drawing of a suitably chosen subtree of  $T$ , which may make the height bound a bit smaller and (as we will see) gives a tight bound.

To explain which subtree of  $T$  we use, we need a few definitions illustrated in Figure 1. Let the *inner skeleton* of a Halin-graph be the tree  $T'$  obtained by deleting all leaves of the skeleton. Define the *leaf-reduction*  $T''$  of  $T'$  as follows. Start with  $T'$ . While there exists a leaf  $\ell$  in the current tree such that the unique neighbour  $p$  of  $\ell$  has degree at most 2, delete  $\ell$  and repeat in the remaining tree. So the leaf-reduction of a path is a single vertex, and the leaf-reduction in general replaces any path of degree-2 vertices that ends at a leaf by a single edge.

We now have the following result:

**Theorem 1** *Let  $H(T)$  be an extended Halin-graph and let  $T''$  be the leaf-reduction of the inner skeleton  $T'$ . If  $T''$  has a plane poly-line drawing  $\Gamma''$  of height  $h$ , then  $H(T)$  has a plane poly-line drawing of height  $3h$ .*

**Proof:** We prove the theorem by giving an algorithm INSERTCYCLEEDGES that converts  $\Gamma''$  into the desired plane poly-line drawing. Figure 3 illustrates the steps of INSERTCYCLEEDGES, with the final result in Figure 1b.

1. As a first step, insert a dummy-vertex at every bend of  $\Gamma''$  to get a straight-line drawing  $\Gamma''_d$  of a tree  $T''_d$  that is tree  $T''$  with some edges subdivided. Also subdivide the same edges in trees  $T'$  and  $T$  to get trees  $T'_d$  and  $T_d$ .

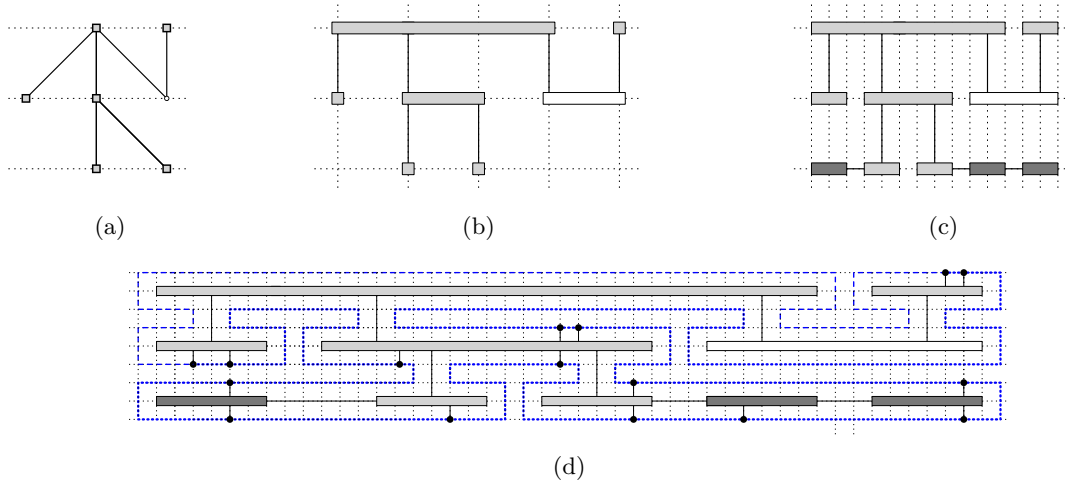


Figure 3: Transform (a) a poly-line drawing of  $T''$  (with a white dummy-vertex inserted at a bend) into (b) a flat visibility representation. (c) Undo the leaf-reduction and widen vertex-segments so that they have no vertical segments at the ends ( $x$ -coordinates are not to scale). Then (d) triple the grid and insert cycle  $C$  and the leaves to get a flat orthogonal drawing (drawn to scale).

2. Next, convert straight-line drawing  $\Gamma''_d$  into a flat visibility representation  $\Gamma''_{vr}$  while maintaining the same height and the ccw orders [3]. This makes all edges horizontal or vertical; we may therefore assume (after enumerating vertical segments left-to-right) that all segments begin and end at integral  $x$ -coordinates.
3. Next, expand visibility representation  $\Gamma''_{vr}$  of  $T''_d$  into a visibility representation  $\Gamma'_{vr}$  of  $T'_d$ . Recall that  $T'_d$  can be obtained from  $T''_d$  by repeatedly adding a leaf  $\ell$  incident to a vertex  $p$  that has degree at most one in the current tree. So the segment  $s(p)$  of  $p$  has (in the current visibility representation) at most one incident horizontal edge segment. If (say) the left side of  $s(p)$  has no incident horizontal edge segment, then insert (if needed) a column left of  $s(p)$  to make space, and then place a (zero-length) segment for  $\ell$  here and connect it horizontally to  $p$ . Repeating this as needed gives a visibility representation  $\Gamma'_{vr}$  of  $T'_d$ . By inserting further columns and extending segments as needed, we may assume that any vertex-segment in  $\Gamma'_{vr}$  has no incident vertical edge-segment in its leftmost and rightmost column.
4. Next, *triple the grid*, i.e., insert a new grid-line before and after each existing one; call the result  $\Gamma'_3$ . Now surround the entire drawing of  $T'_d$  with a cycle  $C$  by tracing along all segments. Formally, take all points that are within  $L_\infty$ -distance 1 of some segment of  $\Gamma'_3$ , and let  $C$  be the boundary of this set. Since we tripled the grid, boundary  $C$  is a single closed poly-line. Let  $\Gamma'_C$  be the drawing where we have added  $C$ .
5. Now we insert the leaves of  $T_d$ . Consider one such leaf  $\ell$  and let  $v$  be its neighbour in the inner skeleton  $T'_d$ . Let  $e, e'$  be the incident edges in  $T'_d$  that are incident to  $v$  and nearest to  $(v, \ell)$  in the ccw order at  $v$  in  $T_d$ . Put differently, edges  $e, e'$  are consecutive at  $v$  in  $T'_d$  and edge  $(v, \ell)$  falls between  $e$  and  $e'$  in the order at  $v$  in  $T_d$ . We say that  $\ell$  belongs to angle  $\langle e, v, e' \rangle$ . Note that  $e = e'$  is possible if  $v$  is a leaf.

Since  $s(v)$  has no incident vertical edge in its first and last column in  $\Gamma'_{vr}$  (hence in the first three and last three columns in  $\Gamma'_3$ ), cycle  $C$  traces parallel to  $s(e)$ , then is within unit distance of  $s(v)$  during a poly-line that include at least one horizontal segment (call it  $s_\ell$ ), and then traces parallel to  $s(e')$ . We place  $\ell$  (and also all other leaves that belong to angle  $\langle e, v, e' \rangle$ ) as points on  $s_\ell$  and connect them vertically to  $s(v)$ . (If needed, we can widen  $s_\ell$  by inserting further columns.)

6. This gives a *flat orthogonal drawing*  $\Gamma_{od}$  of  $T_d$ : every vertex is represented by a horizontal segment, and every edge is a poly-line with only horizontal or vertical segments. Furthermore, the height is  $3h$  and the drawing represents  $H(T_d)$  since we took care to re-insert the leaves exactly according to the planar embedding. Drawing  $\Gamma_{od}$  can be converted to a poly-line drawing  $\Gamma_d$  of  $H(T_d)$  of the same height [3].
7. Finally by reverting dummy-vertices of  $T_d$  back to bends, we obtain the desired poly-line drawing of  $H(T)$ .

□

**Corollary 2** *Any  $n$ -vertex extended Halin-graph  $H(T)$  has a plane poly-line drawing of height  $6pw(T'') + 3 \in O(\log n)$  and width  $O(n)$ , where  $T''$  is the leaf-reduction of the inner skeleton.*

**Proof:** It is known that  $T''$  has a plane straight-line drawing  $\Gamma''$  of height  $2pw(T'') + 1$  [1]. The height of  $\Gamma''$  is  $O(\log n)$  since every tree has pathwidth at most  $\log_3(2n + 1)$  [24].

Now apply algorithm INSERTCYCLEEDGES from Theorem 1 (we re-use the notations defined there). There are no dummy-vertices, so  $T''_d = T''$ . Visibility representation  $\Gamma'_{vr}$  has width  $O(n)$  after deleting redundant columns [3]. Creating  $\Gamma_{od}$  triples the height (so it is at most  $6pw(T'') + 3 \in O(\log n)$ ) and adds at most one column per leaf (keeping the width at  $O(n)$ ). Finally converting a planar flat orthogonal drawing into a planar poly-line drawing increases neither height nor width [3], and so the result follows. □

Our construction may seem very wasteful (the cycle-edges have many bends that could be removed with suitable post-processing stages), but as we shall see in Theorem 9, the height-bound is tight, even for some regular Halin-graphs. We conjecture that the asymptotic bound on the area cannot be improved, but no lower bound (other than the trivial  $\Omega(n)$ ) is known for the area of drawings of Halin-graphs.

Corollary 2 can be seen as an approximation-algorithm for the height.

**Corollary 3** *There exists a linear-time 6-approximation algorithm for the height of a plane poly-line drawing of a Halin-graph.*

**Proof:** Consider a Halin-graph  $H$  and let  $T''$  be the leaf-reduction of its inner skeleton. Any plane drawing  $\Gamma$  of  $H$  induces a plane drawing  $\Gamma''$  of  $T''$ , and  $\Gamma''$  must have height at least  $pw(T'')$  [15]. Furthermore, the cycle-edges of  $H$  surround drawing  $\Gamma''$  since  $\Gamma$  is plane; this requires at least two more units of height [9]. So any plane poly-line drawing of  $H$  has height at least  $pw(T'') + 2$ , and Corollary 2 achieves at most 6 times this bound. One can easily find the drawing in linear time following the steps of the proof. □

Using the same transformation-techniques, we can also get linear-area drawings of Halin-graphs for which the skeleton is balanced in some sense. Define a *complete binary tree* to be a tree where (when rooted suitable) every non-leaf vertex has exactly two children, and all children have the same distance to the root.

**Observation 4** *The Halin-graph for which the skeleton is a complete binary tree has a plane poly-line drawing in  $O(n)$  area.*

**Proof:** The complete binary tree has a so-called *h-v-drawing* of linear area, and specifically, width and height  $O(\sqrt{n})$  [7]. In this drawing, all vertices are points and edges are drawn horizontally or vertically, so the drawing can be viewed as a flat visibility representation with width and height  $O(\sqrt{n})$ . See Figure 4.

Now consider  $H(T)$ , where  $T$  is the complete binary tree, and so is the inner skeleton  $T'$ . Use the h-v-drawing of  $T'$  with width and height  $O(\sqrt{n})$  as a flat visibility representation  $\Gamma'_{vr}$ , and transform it into a poly-line drawings with steps 3-7 of algorithm INSERTCYCLEEDGES. Observe that these steps at most triple the width and height since every leaf of  $T'$  has two attached leaves of  $T$ . Hence the poly-line drawing has width and height  $O(\sqrt{n})$  as desired.  $\square$

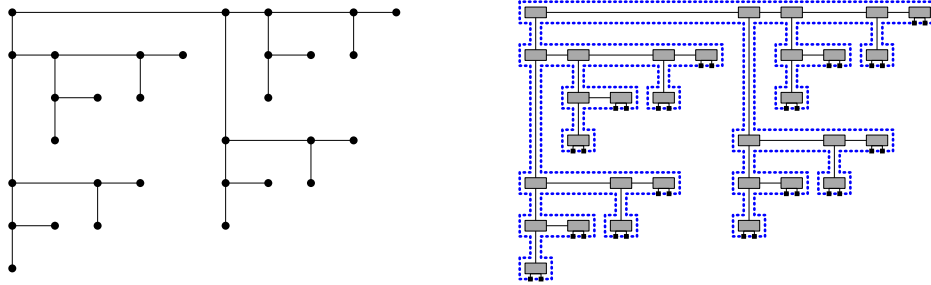


Figure 4: Drawing a complete binary tree in linear area (based on [7]), and drawing  $H(T)$  in linear area if  $T$  is a complete binary tree.

Likewise, the existence of linear-area h-v-drawings of Fibonacci-trees [7] or more generally AVL-trees [8] means that Halin-graphs for which the skeleton is such a tree have linear-area drawings.

## 4 Straight-line drawings

The transformation of Section 3 creates poly-line drawings, and it is not at all clear whether one could convert them into straight-line drawings without changing the height. We hence give a second, completely different algorithm that creates a straight-line plane drawing of a Halin-graph, at the cost of doubling the height. We show the following result:

**Theorem 5** *Every regular Halin-graph  $H(T)$  has a straight-line drawing of height at most  $12pw(T) - 3$ , and every extended Halin-graph  $H(T)$  has a straight-line drawing of height at most  $12pw(T) - 1$ .*

The proof of Theorem 5 will be done via Lemma 1 below. To state this lemma succinctly, we introduce some notation. The *characteristic function*  $\chi(\cdot)$  evaluates to 1 if the expression inside the parentheses is true, and to 0 otherwise. For a tree  $T$ , we use  $\chi_{\text{ext}}(T)$  as a convenient shortcut for

$$\chi\left(H(T) \text{ is an extended Halin-graph and not a regular Halin-graph}\right),$$

i.e.,  $\chi_{\text{ext}}(T)$  is 1 if some vertex of  $T$  has degree 2 and  $\chi_{\text{ext}}(T) = 0$  otherwise. Note that if  $T$  is rooted and  $T'$  is a rooted subtree of  $T$ , then  $\chi_{\text{ext}}(T') \leq \chi_{\text{ext}}(T)$ . We will show the following in Section 4.1:

**Lemma 1** *For any Halin-graph  $H(T)$  where  $T$  has been rooted arbitrarily, there exists a plane flat visibility representation with height at most  $6rpw(T) - 9 + 2\chi_{\text{ext}}(T)$ .*

We now argue that this lemma implies Theorem 5.

**Proof:** (of Theorem 5) Root  $T$  arbitrarily and use Lemma 1 to obtain a plane flat visibility representation  $\Gamma_{vr}$  of  $H(T)$  with height  $6rpw(T) - 9 + 2\chi_{\text{ext}}(T)$ . Transform  $\Gamma_{vr}$  into a plane straight-line drawing  $\Gamma$  of the same height ([3], based on [12, 23]). Since  $rpw(T) \leq 2pw(T) + 1$  [5], drawing  $\Gamma$  has height at most  $12pw(T) + 6 - 9 + 2\chi_{\text{ext}}(T)$ , which implies the result.  $\square$

Similarly as in Corollary 3, one argues that this theorem gives a 12-approximation algorithm on the height of a plane straight-line drawing of a Halin-graph.

### 4.1 Proof of Lemma 1

We first outline the idea for the proof of Lemma 1. We give a recursive algorithm that draws the skirted graph  $H^-(T)$  by combining drawings of skirted graphs of rooted subtrees  $T'$  of  $T$ . We draw tree  $T$  left-to-right, i.e., with parents to the left of their children. To be able to draw edges of  $T$ , we impose that the root of each subtree  $T'$  occupies a point on the left side of the minimum axis-aligned bounding box of the drawing of  $T'$ .

To choose where to merge subtrees at children of the root, we use essentially the idea of Garg and Rusu [21], except rotated by  $90^\circ$  and using a spine-child in place of the child with the largest subtree. Thus, place the spine-child rightmost. All other subtrees are merged somewhere between the root and the spine-child; specifically the left-to-right order contains first the before-spine children, then the after-spine children, and then the spine-child. In particular, the left-to-right order of subtrees does *not* reflect the age-order of the children.

With the drawing of each subtree  $T'$ , we must also consider where to place the *connector-edges* of  $T'$ , i.e., the edges of  $H^-(T)$  that have exactly one endpoint in  $T'$  and the other endpoint in  $T \setminus T'$ . These are the edges from the root of  $T'$  to its parent, as well as the cycle-edges of  $H^-(T)$  (if any) that are incident to the first and last leaf of  $T'$ . Because the left-to-right order of subtrees does not necessarily reflect the age-order of children, we have to permit multiple ways of restricting the location of the first/last leaf of  $T'$  so that we can insert these connector-edges without bends.

**Drawing types:** We construct six different types of drawings for a subtree  $T'$ , denoted LLR-drawing, RLL-drawing, RLR-drawing, LTL-drawing, LLL-drawing and LBL-drawing. The three letters  $\alpha\beta\gamma$  of this drawing-type specify restrictions on the position of the first leaf, the root, and the last leaf of  $T'$ , respectively. To explain these restrictions, we need two notations. We say that (in a flat visibility representation) a vertex  $v$  *occupies point*  $p$  if segment  $s(v)$  includes point  $p$ . Also, we use  $\square(\Gamma)$  to denote the minimum enclosing axis-aligned box of  $\Gamma$ .

**Definition 6** *Let  $T$  be a rooted tree. Let  $\Gamma$  be a plane flat visibility representation of  $H^-(T)$  in layers  $1, \dots, h$  (enumerated top to bottom), for some  $h \geq 2$ . We call  $\Gamma$  an  $\alpha\beta\gamma$ -drawing (where  $\alpha\beta\gamma$  is any of the combinations LLR, RLL, RLR, LTL, LLL, LBL) if it satisfies the following (see also Figure 5):*

- *If  $\alpha = \text{L}$ , then the first leaf occupies the bottom left corner of  $\square(\Gamma)$ . Otherwise ( $\alpha = \text{R}$ ) it occupies some point on the right side of  $\square(\Gamma)$ .*
- *Root  $r$  occupies some point on the left side of  $\square(\Gamma)$ . If  $\beta = \text{T}$ , then the root  $r$  is in layer 2. If  $\beta = \text{B}$ , then  $r$  is in layer  $h - 1$ . Otherwise ( $\beta = \text{L}$ )  $r$  can be in any layer.*

- If  $\gamma = L$ , then the last leaf occupies the top left corner of  $\square(\Gamma)$ . Otherwise ( $\gamma = R$ ) it occupies some point on the right side of  $\square(\Gamma)$ .

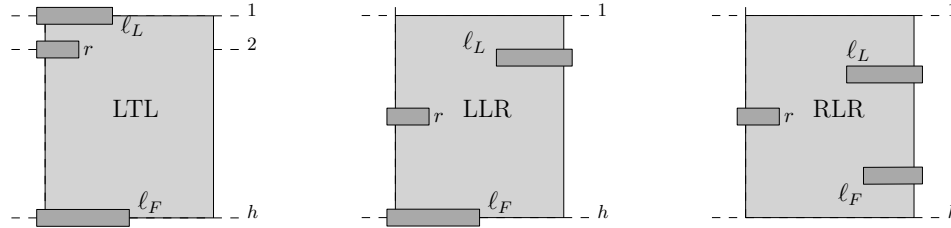


Figure 5: Drawing types restrict the location of the first leaf  $\ell_F$ , the root  $r$  and the last leaf  $\ell_L$ .

**Modifying drawings:** To reduce the number of cases, we use a known method to modify a flat visibility representation (see e.g. [2]). We revisit its details here because we must study how the modification affects the drawing type.

**Claim 7** Assume that  $H^-(T)$  has an  $L\beta L$ -drawing  $\Gamma$  of height  $h \geq 2$  for some  $\beta \in \{T, B, L\}$ . Then for any  $\alpha, \gamma \in \{L, R\}$  it also has an  $\alpha L\gamma$ -drawing  $\Gamma'$  of height  $h + \chi(\alpha=R) + \chi(\gamma=R)$ . Furthermore, the first and last leaf are in the bottom and top layer of  $\square(\Gamma')$ , respectively.

**Proof:** Figure 6a illustrates the transformation. The last leaf  $\ell_L$  is in the topmost layer of  $\square(\Gamma)$  since it is in L-position and hence occupies the top-left corner. To achieve  $\gamma = R$ , add a new layer above  $\square(\Gamma)$ , move  $\ell_L$  into it, and expand it rightwards over the entire width of  $\square(\Gamma)$ . Its incident vertical edges can simply be extended, while its incident horizontal edge (if any) can be re-routed vertically. This leaves the bottom layer unchanged, so the first leaf  $\ell_F$  retains its L-position. The root  $r$  loses the T-position (if it was in it), but this is not a problem since we only promised an L-position for the root in  $\Gamma'$ . Similarly one achieves  $\alpha = R$  by adding a layer below  $\square(\Gamma)$  and moving  $\ell_F$  into it.  $\square$

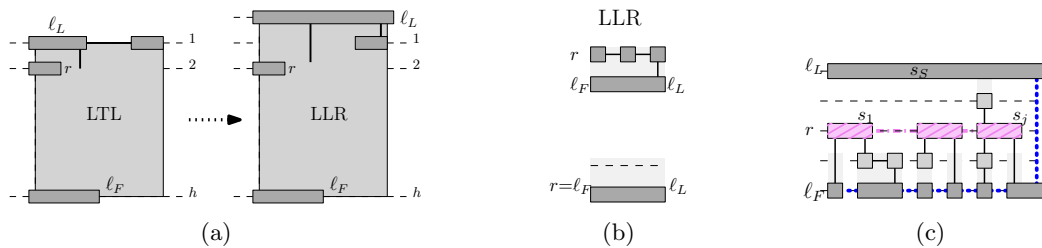


Figure 6: (a) Achieving  $\gamma = R$ . (b) Drawings of height 2 if  $rpw(T) = 1$ . (c) The case  $rpw(T) = 2$ . Path  $P'$  is purple (dash-dotted, with upward striped vertex-boxes), degree-2 vertices are light gray, cycle-edges are blue (thick dotted). Bounding boxes of subtree-drawings are lightly shaded.

So if we have a method to create an LTL-drawing, then by using the claim we can convert it into drawings of type RLL, LLR or RLR by adding one or two layers. The method can also be used for creating LBL-drawings via the *reversal trick*: Consider the tree  $T^{\text{rev}}$  where all orders of

all children have been reversed. Create an LTL-drawing of  $H^-(T^{\text{rev}})$ , and flip it upside-down to obtain an LBL-drawing of  $H^-(T)$ . Hence, due to Claim 7, we will mostly only study how to create LTL-drawings.

**The special cases  $\text{rpw}(T) \leq 2$ :** If the rooted pathwidth of  $T$  is small, then we only construct drawings for a subset of the six types defined earlier. For  $\text{rpw}(T) = 1$  this is a necessity, since not all drawing types can exist when the first and last leaf are identical. For  $\text{rpw}(T) = 2$  this improves the height-bound slightly.

**Lemma 2** *Let  $T$  be a rooted ordered tree with  $\text{rpw}(T) = 1$  and let  $\alpha\beta\gamma$  be either LLR or RLL. Then  $H^-(T)$  has a plane  $\alpha\beta\gamma$ -drawing of height exactly 2. Furthermore, the unique leaf occupies an entire layer of the drawing.*

**Proof:** We only explain how to create the LLR-drawing; the other case is symmetric. The tree is a rooted path ending at the unique leaf  $\ell_F = \ell_L$ . Place the leaf on layer 2 and the path to the leaf (if any) on layer 1, in order and with the root leftmost. See Figure 6b. Note that if  $T$  is a single vertex, then we intentionally include an empty layer in the drawing to achieve height exactly 2. One verifies all restrictions on the drawing-type; here it is crucial that the R-position permits *any* point on the right side for  $\ell_L$ .  $\square$

**Lemma 3** *Let  $T$  be a rooted ordered tree with  $\text{rpw}(T) = 2$ , and let  $\alpha\beta\gamma$  be any of the combinations LLR, RLL, RLR, and LLL. Then  $H^-(T)$  has a plane  $\alpha\beta\gamma$ -drawing of height at most  $6\text{rpw}(T) - 9 + \chi(\alpha=R) + \chi(\gamma=R) + 2\chi_{\text{ext}}(T)$ .*

**Proof:** We only explain how to construct an LLL-drawing, the other drawing-types are achieved using Claim 7. Consider Figure 6c. Fix 5 layers and a spine  $P = \langle s_1, \dots, s_S \rangle$  that goes from root to a leaf. Let  $j$  be maximal such that  $s_j$  has at least two children; by  $\text{rpw}(T) > 1$  such an index exists. Place  $P' := \langle s_1, \dots, s_j \rangle$  on layer 3, with the root  $s_1$  leftmost.

Any subtree  $T' \in \mathcal{T}(T, P')$  has rooted pathwidth 1 since  $P$  is a spine and  $j$  was chosen maximal. The root  $r'$  of  $T'$  is a child of some spine-vertex; if it is an after-spine child or the last child of  $s_j$ , then use Lemma 2 to obtain an RLL-drawing of  $T'$ , else obtain an LLR-drawing of  $T'$ . Place this drawing in the two layers above respectively below  $P'$ , respecting the order of children. The cycle-edges can now be drawn horizontally along layers 1 and 5, with the exception of the cycle-edge that connects two leaves that are descendants of the next-to-last child and last child of  $s_j$ , respectively. Since those leaves occupy the entire layer in their respective drawings, they can be expanded rightward and the cycle-edge can then be drawn with a vertical segment on the right. The first and last leaf of  $T$  are leftmost in the bottom and top layer, so after expanding them leftward, if needed, they occupy the leftmost corners of the bounding box.

This gives an LLL-drawing of height 5. If  $\chi_{\text{ext}}(T) = 0$  then any subtree  $T' \in \mathcal{T}(T, P')$  consists of a single vertex. Therefore layers 2 and 4 contain no horizontal segment and can be deleted to obtain height 3. So we get an LLL-drawing of height  $3 + 2\chi_{\text{ext}}(T) = 6\text{rpw}(T) - 9 + 2\chi_{\text{ext}}(T)$ .  $\square$

**The induction hypothesis:** We create drawings for larger rooted pathwidth using induction; the following states the induction hypothesis. (It differs from Lemma 3 only in that LTL-drawings and LBL-drawings are also permitted.)

**Lemma 4** *Let  $T$  be a rooted ordered tree with  $\text{rpw}(T) \geq 3$ , and let  $\alpha\beta\gamma$  be any of the combinations LLR, RLL, RLR, LLL, LTL and LBL. Then  $H^-(T)$  has a plane  $\alpha\beta\gamma$ -drawing of height at most  $6\text{rpw}(T) - 9 + \chi(\alpha=R) + \chi(\gamma=R) + 2\chi_{\text{ext}}(T)$ .*

Before proving this lemma, we observe that it implies Lemma 1. Namely, take an LLL-drawing  $\Gamma$  of  $H^-(T)$  obtained by Lemma 3 or 4. (We know  $rpw(T) \geq 2$  since  $T$  was assumed to have at least three leaves when unrooted.) Drawing  $\Gamma$  has height at most  $6rpw(T) + 9 + 2\chi_{\text{ext}}(T)$ . To complete this into a drawing of  $H(T)$ , we must either add edges  $(r, \ell_F)$  and  $(r, \ell_L)$  (if the root is a leaf) or add edge  $(\ell_F, \ell_L)$ . But in an LLL-drawing vertices  $\ell_F, r, \ell_L$  all occupy points on the left side; by extending their segments leftward we can add the missing edges vertically and obtain the desired visibility representation for Lemma 1.

To prove Lemma 4, it suffices to show how to construct an LTL-drawing as discussed above. We use the following notations throughout. Let  $r$  be the root of  $T$ , let  $d$  be its degree, and let  $c_1, \dots, c_d$  be the children of the root, in age-order. Let  $\ell_F^i$  and  $\ell_L^i$  (for  $i = 1, \dots, d$ ) be the first and last leaf of the rooted subtree  $T_{c_i}$ . Let  $c_s$  be a child of  $r$  that maximizes  $rpw(T_{c_s})$ ; this belongs to a spine [5], and therefore

$$rpw(T_{c_i}) < rpw(T) \quad \text{for all } i \neq s. \tag{1}$$

If  $rpw(T_{c_s}) < rpw(T)$  then (to avoid some cases) we re-assign  $s := d$ ; note that this does not affect the validity of (1).

We prove Lemma 4 by induction on  $rpw(T)$ . We know that  $rpw(T) \geq 3$ , so the base case is  $rpw(T) = 3$ . We do an inner induction on the size of the tree, and use as base case for the inner induction that  $rpw(T_{c_s}) < 3$ . Much of the construction will be the same for base case and induction step, and we therefore prove them together.

**Drawing subtrees up to the spine-child:** We build the drawing left-to-right, beginning with the root and then adding the subtrees at the children. See also Figure 7.

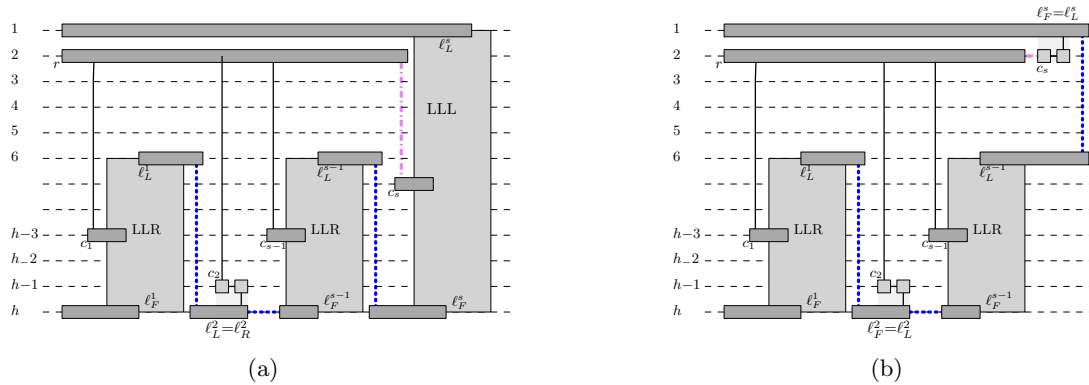


Figure 7: The constructions if the spine-child is the last child. We also illustrate some subtrees that have rooted pathwidth 1 ( $T_{c_2}$  in both figures, and  $T_{c_s}$  on the right).

1. Define  $h := 6rpw(T) - 9 + 2\chi_{\text{ext}}(T) \geq 9$  and create  $h$  layers, enumerated from top to bottom. If we can argue that our constructed drawing  $\Gamma$  fits within these layers, then the height-bound for Lemma 4 holds.
2. [Handle the root]
 

Place the segment  $s(r)$  for root  $r$  in layer 2, with its left endpoint fixed (this will be the left side of the bounding box of our drawing), while its right endpoint remains unfixed for now.

Put differently, we think of  $s(r)$  as expanding rightward with each of the following steps. We will stop expanding  $s(r)$  when adding the last child  $c_d$ , which happens either in Step 4 or in Step 8.

3. [Handle the before-spine children]

For  $i = 1, \dots, s - 1$ , let  $\Gamma_i$  be an LLR-drawing of  $H^-(T_{c_i})$ . This can be obtained recursively if  $rpw(T_{c_i}) \geq 3$  and via Lemma 2 or 3 otherwise. We claim that  $\Gamma_i$  has height at most  $h - 5$ . This is obvious if  $rpw(T_{c_i}) = 1$  since then  $\Gamma_i$  has height  $2 \leq h - 5$  by  $h \geq 9$ . Otherwise  $\Gamma_i$  has height at most  $6rpw(T_{c_i}) - 9 + 1 + 2\chi_{\text{ext}}(T_{c_i})$ . Since  $rpw(T_{c_i}) \leq rpw(T) - 1$  by (1) and  $\chi_{\text{ext}}(T_{c_i}) \leq \chi_{\text{ext}}(T)$ , this is at most  $6rpw(T) - 6 - 9 + 1 + 2\chi_{\text{ext}}(T) = h - 5$ . Place  $\Gamma_i$  in layers  $6, \dots, h$ , to the right of everything drawn thus far and aligned to the bottom if its height is less than  $h - 5$ .

Recall that we must draw the connector-edges of  $T_{c_i}$ , i.e., the edge  $(r, c_i)$  as well as the cycle-edges (if any) connecting  $\ell_F^i$  and  $\ell_L^i$  to the leaves at the older/younger sibling. We draw these as follows:

- Vertex  $c_i$  occupies a point on the left side of  $\square(\Gamma_i)$ . Since the segment of  $r$  extends rightward as needed, we can hence add a vertical segment for  $(c_i, r)$  after expanding (if needed) the segment of  $c_i$  slightly leftward beyond  $\square(\Gamma_i)$ .
- Leaf  $\ell_F^i$  occupies the bottom-left corner of  $\square(\Gamma_i)$  and is hence placed in layer  $h$  of  $\Gamma$ . For  $i = 1$ , leaf  $\ell_F^i$  is the first leaf of  $T$ ; expand its segment leftward within layer  $h$  until it occupies the bottom-left corner of  $\square(\Gamma)$ . For  $i > 1$ , we need to create a segment for connector-edge  $(\ell_L^{i-1}, \ell_F^i)$ . Observe that  $\ell_L^{i-1}$  is on the right side of  $\square(\Gamma_{i-1})$  while  $\ell_F^i$  is on the left side of  $\square(\Gamma_i)$ , and these two bounding boxes are next to each other. If  $\ell_L^{i-1}$  and  $\ell_F^i$  are in the same layer, then we can connect them horizontally. Otherwise, expand  $\ell_L^{i-1}$  rightward and  $\ell_F^i$  leftward until they can be connected with a vertical segment.
- Connector-edge  $(\ell_L^i, \ell_F^{i+1})$  will be drawn when handling  $c_{i+1}$ .

4. [Handle the spine-child if  $s = d$ ]

We have three cases for the spine-child  $c_s$ . Assume first that  $s = d$  and  $rpw(T_{c_s}) \geq 2$  and consider Figure 7a. Recursively (or via Lemma 3) obtain an LLL-drawing  $\Gamma_s$  of  $H^-(T_{c_s})$ . This has height at most  $h$  by  $rpw(T_{c_s}) \leq rpw(T)$ . Place  $\Gamma_s$  in layers  $1, \dots, h$ , top-aligned and to the right of everything drawn thus far (thus also ending the segment of  $r$ ). Connector-edges  $(c_s, r)$  and  $(\ell_L^{s-1}, \ell_F^s)$  can be completed as in Step 3. Leaf  $\ell_L^s$  is the last leaf of  $T$  and in layer 1; we can expand its segment leftward in layer 1 to occupy the top left corner of  $\square(\Gamma)$ .

Assume next that  $s = d$  and  $rpw(T_{c_s}) = 1$ . (This can happen even though  $rpw(T) \geq 3$  if we re-assigned  $s$ .) See also Figure 7b. In this case there is no LLL-drawing of  $T_{c_s}$ , but we use instead the RLL-drawing  $\Gamma_s$  of  $T_{c_s}$  from Lemma 2. Place it in layers 1 and 2 (thus also ending the segment of  $r$ ). Edge  $(r, c_s)$  can be drawn (normally horizontally, but vertically if  $T_{c_s}$  has only one vertex). To route connector-edge  $(\ell_L^{s-1}, \ell_F^s)$ , extend both  $\ell_F^s$  and  $\ell_L^{s-1}$  rightward beyond  $\square(\Gamma_s)$  and add a vertical segment; this is feasible since  $\ell_L^{s-1}$  is in R-position and not in layer 1 or 2, while  $\ell_F^s$  occupies all of layer 1 in  $\Gamma_s$ . Leaf  $\ell_L^s$  can again be expanded leftward to occupy the top left corner.

Assume finally that  $s < d$ , i.e., the spine-child is not the last child of the root. The drawing here is more complicated; the algorithm continues with Step 5 below.

Our construction is done if  $s = d$ , so assume otherwise. This implies that  $rpw(T_{c_s}) = rpw(T)$ , for otherwise we would have re-assigned  $s$  to be  $d$ . So  $rpw(T_{c_s}) \geq 3$ , which means that we are not in the base case of the inner induction. (Put differently, in the base case Step 4 finishes the construction.) Crucially, by  $rpw(T_{c_s}) \geq 3$  we can apply induction, rather than Lemma 2 or 3, and use an LBL-drawing for the spine-child. This in turn permits us to route  $(r, c_s)$  while leaving sufficiently much space for the after-spine children. We first explain this in the case  $s \leq d - 2$ ; the case  $s = d - 1$  needs a minor variation that will be given later.

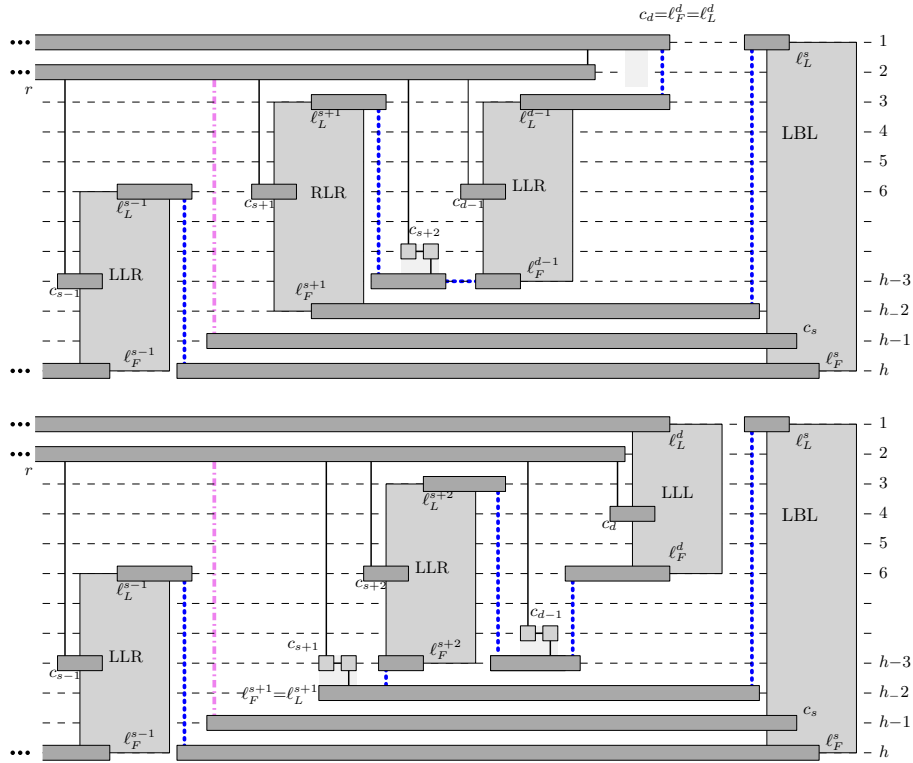


Figure 8: (Top) The rest of the construction if  $s \leq d - 2$ . (Bottom) The construction again, with other subtrees that have rooted pathwidth 1.

**The case  $s \leq d - 2$ :** If  $s \leq d - 2$ , then continue building the drawing as follows (see also Figure 8):

5. [Draw some connector-edges for the spine-child]

Place segments in layers  $h - 1$  and  $h$  for  $c_s$  and  $\ell_F^s$ , respectively; they begin to the right of everything drawn thus far and will continue to expand rightward until Step 9. Draw  $(r, c_s)$  vertically. Draw connector-edge  $(\ell_L^{s-1}, \ell_F^s)$  similarly as in Step 3: horizontally if  $\ell_L^{s-1}$  is in layer  $h$  and vertically (after expanding the segments slightly) otherwise.

6. [Handle the first after-spine child]

Let  $\Gamma_{s+1}$  be an RLR-drawing of  $H^-(T_{c_{s+1}})$ . If  $rpw(T_{c_{s+1}}) \geq 2$ , then this can be obtained recursively or via Lemma 3. If  $rpw(T_{c_{s+1}}) = 1$ , then use as  $\Gamma_{s+1}$  the LLR-drawing of Lemma 2; this is also an RLR-drawing since the unique leaf of  $T_{c_{s+1}}$  occupies all of layer 2 in  $\Gamma_{s+1}$ . Similarly as in Step 3 one argues that drawing  $\Gamma_{s+1}$  has height at most  $h - 4$ . Place  $\Gamma_{s+1}$  in layers  $3, \dots, h - 2$ , bottom-aligned and to the right of everything drawn thus far. Connector-edge  $(r, c_{s+1})$  can be drawn vertically, the other two connector-edges will be drawn when handling  $c_{s+2}$  and  $c_s$ , respectively.

We crucially need that  $\ell_F^{s+1}$  occupies the entire bottom layer of  $\square(\Gamma_{s+1})$ . This is not guaranteed by its R-position alone, but holds if  $rpw(T_{c_{s+1}}) \geq 2$ , because then  $\Gamma_{s+1}$  was obtained via Claim 7. It also holds if  $rpw(T_{c_{s+1}}) = 1$  since then  $\ell_F^{s+1}$  occupies the entire bottom layer of  $\square(\Gamma_s)$ . Thus  $\ell_F^{s+1}$  (which is placed in layer  $h - 2$ ) can in future steps expand its segment rightward as needed (it will be completed in Step 9).

7. [Handle more after-spine children]

For  $i = s + 2, s + 3, \dots, d - 1$ , we process  $H^-(T_{c_i})$  and its connector-edges as we did in Step 3, only we put the drawing three levels higher to reside in layers  $3, \dots, h - 3$ .

One special situation occurs for  $i = s + 2$  if  $T_{c_{s+1}}$  was a rooted path. In this case,  $\ell_L^{s+1}$  equals  $\ell_F^{s+1}$  and was placed in layer  $h - 2$  and extended rightward, hence is *below*  $\square(\Gamma_{s+2})$  rather than to its left. But we can then draw connector-edge  $(\ell_L^{s+1}, \ell_F^{s+2})$  by going downward from  $\ell_F^{s+2}$ .

8. [Handle the last child]

We process  $T_{c_d}$  very similarly to Step 4, by using an LLL-drawing (if  $rpw(T_{c_d}) \geq 2$ ) and an LLR-drawing otherwise. This drawing  $\Gamma_d$  has height at most  $h - 6$  by  $rpw(T_{c_d}) < rpw(T)$  and  $h \geq 9$ . Place  $\Gamma_d$  in layers  $1, \dots, h - 6$ , top-aligned; this ends the segment of  $r$ . Vertex  $\ell_L^d$  is the rightmost leaf of  $T$ ; expand its segment leftward in layer 1 to occupy the top left corner. Connector-edges  $(r, c_d)$  and  $(\ell_L^{d-1}, \ell_F^d)$  are routed as in Step 4.

9. [Handle the spine-child if  $s < d$ ]

Finally, recursively obtain an LBL-drawing  $\Gamma_s$  of  $H^-(T_{c_s})$ . This has height at most  $h$  by  $rpw(T_{c_s}) \leq rpw(T)$ . Place  $\Gamma_s$  to the right of everything drawn thus far, bottom-aligned; this ends the segment of  $\ell_F^{s+1}$  (in layer  $h - 2$ ) and completes the segments of  $c_s$  and  $\ell_F^s$  (in layers  $h - 1$  and  $h$ , respectively). Connector-edge  $(\ell_F^{s+1}, \ell_L^s)$  can be drawn vertically after expanding  $\ell_L^s$  leftward slightly beyond  $\square(\Gamma_s)$ ; the other two connector-edges have already been drawn in Step 5.

This ends the construction in the case  $s \leq d - 2$ .

**The case  $s = d - 1$ :** In Steps 6 and 8 we used an RLR-drawing  $\Gamma_{s+1}$  for  $c_{s+1}$  and an LLL-drawing  $\Gamma_d$  for  $c_d$ . If  $s = d - 1$ , then one drawing must take on both of these roles. To achieve this, replace Steps 6-8 by the following:

6'. [Handle the unique after-spine child if  $s = d - 1$ ]

Let  $\Gamma_d$  be an RLL-drawing for  $H^-(T_{c_d})$ ; this can be obtained recursively or via Lemma 2 or 3. Similarly as in Step 3 one argues that  $\Gamma_d$  has height at most  $h - 5$ . Place  $\Gamma_d$  in layers  $1, \dots, h - 5$ , top-aligned. Vertex  $\ell_L^d$  is expanded leftward and edge  $(r, c_d)$  is routed as in Step 8. Connector-edge  $(\ell_F^{s-1}, \ell_L^s)$  will be drawn in Step 9, though it is now drawn horizontally if  $T_{c_d}$  is a rooted path. See Figure 9.

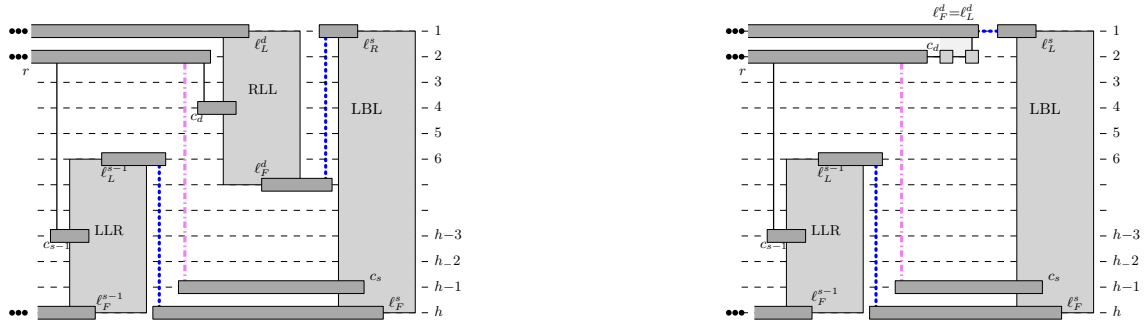


Figure 9: The constructions if  $s = d - 1$ , for  $rpw(T_{c_d}) \geq 2$  and  $rpw(T_{c_d}) = 1$ .

In all cases we have constructed an LTL-drawing. We used  $h = 6rpw(T) - 9 + 2\chi_{\text{ext}}(T) \geq 9$  layers and argued that all drawings of subgraphs fit within this space. Hence Lemma 4 holds. As discussed earlier this implies Lemma 1 and Theorem 5.

It is worth mentioning that this visibility representation can easily be found in linear time, as long as coordinates of vertices are expressed initially via offsets to their parents, and evaluated to their final value only after finishing the construction of the entire drawing.

### 4.2 Halin-graphs with maximum degree 3

Observe that in Figures 7 and 9 (where  $s \in \{d-1, d\}$ ) there are three layers that have no horizontal segments in them and so would not have been needed. This leads to the following.

**Lemma 5** *Let  $T$  be a rooted binary tree with  $rpw(T) \geq 2$ . Then  $H^-(T)$  has a plane LLL-drawing of height  $3rpw(T) - 3 + \chi_{\text{ext}}(T)$ . If  $rpw(T) \geq 3$ , then it has a plane LTL-drawing of the same height.*

**Proof:** We only sketch the necessary changes to the previous proof here; the reader should be able to fill in the details using Figure 10.

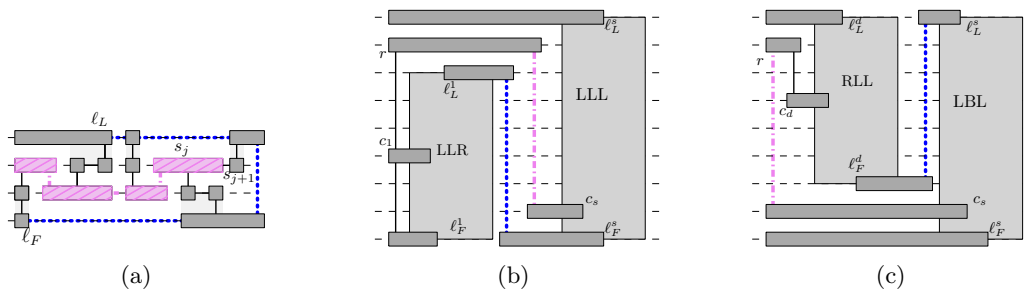


Figure 10: The constructions if the maximum degree is 3.

Consider first the case  $rpw(T) = 2$ . If  $\chi_{\text{ext}}(T) = 0$ , then Lemma 3 gives  $3 = 3rpw(T) - 3 + \chi_{\text{ext}}(T)$  layers as desired. If  $\chi_{\text{ext}}(T) = 1$ , then we want a drawing on four layers. Consider Figure 10a. Let  $P' = \langle s_1, \dots, s_j \rangle$  be as in the proof of Lemma 3. Draw  $P'$  from left to right, with  $s_i$  (for  $1 \leq i \leq j$ ) on layer 2 if it has a before-spine child, and on layer 3 otherwise, and connect edges of  $P'$  horizontally or vertically. Since  $T$  is binary, each non-spine child is the *unique*

non-spine child of its parent, and this placement leaves two layers above or below its parent free for placing the drawing of the subtree. For the spine-child  $s_{j+1}$ , we re-use the layer of  $s_j$  and place the drawing of  $T_{s_{j+1}}$  to the right of  $s_j$ . Cycle-edges can be connected as in Lemma 3.

For  $rpw(T) \geq 3$ , we create the drawing recursively as before. The key difference is that we have  $d \leq 2$  children and hence one of  $s = d$  or  $s = d - 1$  always applies. So construct a drawing of  $H^-(T)$  as in Figure 7 or Figure 9, except use  $h = 3rpw(T) - 3 + \chi_{\text{ext}}(T)$  and in Step 3 place drawing  $\Gamma_i$  for  $i < s$  in layers  $3, \dots, h$ . See Figure 10b and 10c.  $\square$

If a Halin-graph has maximum degree 3, then its skeleton  $T$  is binary when rooting it at a leaf. Taking the LLL-drawing of  $H^-(T)$  from Lemma 5 and expanding it to a drawing of  $H(T)$  as in the proof of Theorem 5 gives:

**Theorem 8** *Every Halin-graph  $H(T)$  with maximum degree 3 has a straight-line drawing of height at most  $6pw(T) + \chi_{\text{ext}}(T)$ .*

## 5 Lower bounds on the height

Both papers that gave approximation algorithms for the height on tree drawings [1, 27] also constructed trees where this bound is tight. In particular, Batzill and the first author showed that there exists an ordered tree that requires height  $2pw(T) + 1$  in any plane drawing [1]. In the same spirit, we now construct Halin-graphs that need as much height as we achieve with our algorithms and show:

**Theorem 9** *There exists a regular Halin-graph  $H(T)$  such that any planar poly-line drawing of  $H(T)$  requires at least  $6pw(T'') + 3$  layers, where  $T''$  is the reduced tree of the inner skeleton of  $H(T)$ .*

Theorem 9 shows that the height-bound in Theorem 1 is tight. We can also show that Lemma 1 is tight; recall that this lemma gave constructions where the height depends on the rooted path-width of the skeleton. Given an unrooted tree  $T$ , define  $rpw_{\min}(T)$  to be the minimum rooted pathwidth over all choices of the root of  $T$ .

**Theorem 10** *There exists a regular Halin-graph  $H(T)$  such that any planar poly-line drawing of  $H(T)$  requires at least  $6rpw_{\min}(T) - 9$  layers.*

**Theorem 11** *There exists an extended Halin-graph  $H(T)$  such that any planar poly-line drawing of  $H(T)$  requires at least  $6rpw_{\min}(T) - 7$  layers.*

All three lower bounds hold even for drawings that do not necessarily respect the planar embedding. The Halin-graphs for all three results are derived from the following trees:

**Definition 12** *For  $w \geq 1$ , define rooted trees  $C_w$  and  $F_w$  together with their spines as follows:*

- $C_1$  consists of an edge  $(r, c)$ , where  $r$  is the root and path  $\langle r, c \rangle$  is the spine. Add a before-spine and an after-spine child at  $r$ , and add two children at  $c$ . See Figure 11a.
- $F_w$  is obtained from  $C_w$  as follows. Let  $r$  be the root of  $C_w$ . Add a parent  $p$  and a grandparent  $g$  to  $r$ , make  $g$  the root, and let the spine of  $F_w$  be the spine of  $C_w$  plus path  $\langle r, c, g \rangle$ . At each of  $g, p$ , add a before-spine and an after-spine child. See Figure 11b.

- $C_{w+1}$  is obtained as follows. Start with the spine, which is a path  $(s_1, \dots, s_S)$  for some sufficiently large constant  $S$  that we will specify later, and make  $s_1$  the root. At each  $s_i$  for  $i \neq S$ , add  $D$  before-spine children and  $D$  after-spine children, for some sufficiently large constant  $D$  that we will specify later. Then make each of these children the root of a copy of  $F_w$ . See Figure 11c.

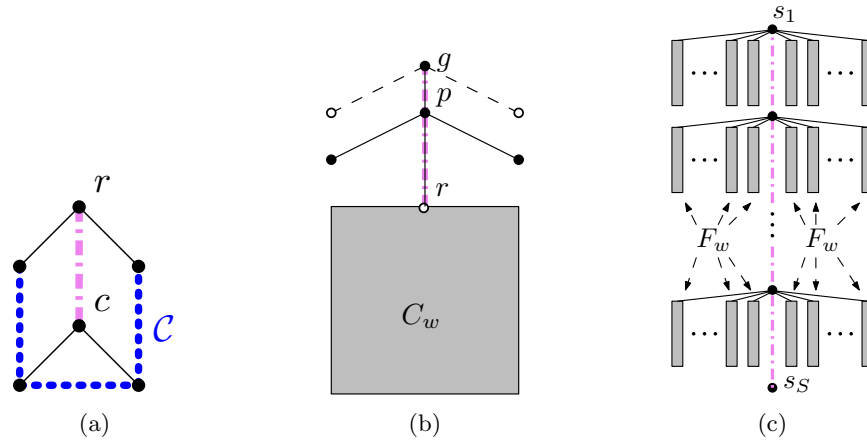


Figure 11: (a)  $C_1$  and its skirted graph. (b) Obtaining  $F_w$  from  $C_w$ . Dashed edges only exist to make the Halin-graph regular. (c) Obtaining  $C_{w+1}$  from many copies of  $F_w$ . As always, cycle-edges are blue (thick dotted) and spine-edges are purple (dash-dotted).

With the above trees we have defined a spine; as we will see in Observation 23 these are indeed spines for purposes of the rooted pathwidth. Define  $h(w) := 6w - 3$ . We will show the following (and argue in Section 5.5 that it implies the theorems):

**Lemma 6** *For  $w \geq 1$ , any plane poly-line drawing of  $H^-(C_w)$  uses at least  $h(w)$  layers.*

### 5.1 Base case and outline

We will prove Lemma 6 by induction on  $w$ . In the base case ( $w = 1$ ) vertex  $c$  in  $C_1$  is surrounded by a 5-cycle  $\mathcal{C}$  in  $H^-(C_1)$ , consisting of the cycle-edges and the edges from root to the first and last leaf. See Figure 11a. Since we need one layer for  $c$ , and two more layers to surround it, any plane drawing of  $H^-(C_1)$  requires three layers, which proves the result by  $h(1) = 3$ .

The induction step will be proved over the next three subsections, but we sketch here the main idea. Fix an arbitrary plane poly-line drawing  $\Gamma$  of  $H^-(C_{w+1})$  for some  $w \geq 1$ . Tree  $C_{w+1}$  contains lots of copies of  $F_w$ . Therefore,  $\Gamma$  contains lots of copies of  $H^-(F_w)$ ; each of them contains a copy of  $H^-(C_w)$  and therefore uses at least  $h(w)$  layers by induction.<sup>2</sup>

We want to show that  $\Gamma$  uses at least  $h(w+1) = h(w)+6$  layers, and to do so, use two major insights. First, while every copy of  $H^-(F_w)$  uses at least  $h(w)$  layers, we can argue that there must exist one copy of  $H^-(F_w)$  that actually uses at least  $h(w) + 1$  layers for its drawing. Since  $H^-(F_w)$  is a connected graph, therefore within its drawing there exists a poly-line  $\hat{\pi}$  that spans  $h(w)+1$  layers.

<sup>2</sup>To keep wordings simpler we often write “ $H^-(C_w)$ ” rather than “a drawing of  $H^-(C_w)$ ”.

The second major insight is that we can find five interior-disjoint poly-lines inside  $\Gamma$  that are disjoint from  $\hat{\pi}$  and that “bypass” it in some sense (see Figure 12 and Definition 14). It is known that five bypassing poly-lines need five additional layers. Therefore the height is at least  $h(w) + 1 + 5 = h(w+1)$ .

Both the existence of  $\hat{\pi}$  and the existence of the five bypassing poly-lines are non-trivial. We therefore structure our proof as follows. We first explain some conventions and how to preprocess the drawing (Section 5.2). We then initially simply assume the existence of  $\hat{\pi}$ , and also make some assumptions on the layout of some subtrees; this makes finding the five bypassing paths very easy (Section 5.3). Two of the assumptions are easily shown to hold by symmetry if  $D$  and  $S$  are big enough (Section 5.4.1 and 5.4.2), but for the other two we need a complicated argument and in particular the distinction between  $C_w$  and  $F_w$  (Section 5.4.3 and 5.4.4; the main argument is in Claim 21).

## 5.2 Preliminaries and preprocessing

So assume that  $w \geq 1$  is fixed and let  $\Gamma$  be an arbitrary plane poly-line drawing of  $H^-(C_{w+1})$ . Enumerate the layers of  $\Gamma$ , from top to bottom, as  $1, 2, \dots, h$ ; we want to show that  $h \geq h(w+1) = h(w) + 6$ . Assume for contradiction that  $h < h(w) + 6$ . We may then assume that  $h = h(w) + 5$  by integrality and because we can add empty layers to  $\Gamma$ . For two points  $p, q$ , we write  $p \prec q$  (or “ $p$  is left of  $q$ ”) if  $p$  and  $q$  are on the same layer and  $p$  has smaller  $x$ -coordinate. Point  $p$  is between  $q_1$  and  $q_2$  is  $q_1 \prec p \prec q_2$  or  $q_2 \prec p \prec q_1$ . We also need the notation of a *polyline*  $\pi$  within drawing  $\Gamma$ ; this is a poly-line that is a subset of the poly-lines used for edges in  $\Gamma$ . In particular, if we fix any two points  $p, q$  of  $\Gamma$ , then there exists a poly-line within  $\Gamma$  that connects  $p$  and  $q$ , since  $\Gamma$  depicts a connected graph. A layer of  $\Gamma$  is identified by its number  $\ell$ , but slightly abusing notation we also use  $\ell$  for the set of points that belong to the layer so that we can write  $\pi \cap \ell$  for the set of points that belong to both  $\ell$  and a poly-line  $\pi$ .

A few minor modifications to drawing  $\Gamma$  will make later arguments easier and do not affect the height. First, insert a bend into any edge-segment that crosses a layer without having a bend there. Second, do the following for any spine-vertex  $s_i$  (with  $i < S$ ) of  $C_{w+1}$ , and any non-spine child  $g$  of  $s_i$ . Recall that  $g$  is the root of a copy of  $F_w$  and has three children; the first and last child are leaves. Delete the two edges to these leaves; their sole purpose was to ensure that the Halin-graph  $H(C_{w+1})$  is regular and they will not be used in the proof below. With this,  $g$  now has degree 2. For the third modification, if  $(s_i, g)$  is not drawn straight-line, then move  $g$  to the bend on  $(s_i, g)$  nearest to  $s_i$ . This makes  $(s_i, g)$  a straight-line segment that (by the first step) crosses no layer. So we may assume the following:

**Observation 13** *Let  $s_i$  (for some  $i < S$ ) be a spine-vertex on layer  $\ell$  (for some  $1 \leq \ell \leq h$ ), and let  $g$  be a non-spine child of  $s_i$ . Then  $g$  is in one of the layers  $\ell-1, \ell$  or  $\ell+1$ , and  $(s_i, g)$  is drawn as a straight-line segment.*

Recall that any non-spine child  $g$  of a spine-vertex  $s_i$  is the root of a copy of  $F_w$ ; we use  $F(g)$  to denote this copy and  $\Gamma(g)$  for the drawing of  $H^-(F(g))$  induced by  $\Gamma$  (after pre-processing). Since  $\Gamma(g)$  contains a drawing of  $H^-(C_w)$  within, it must use at least  $h(w)$  layers by induction. We call  $g$  a *good child* of  $s_i$  if  $\Gamma(g)$  does not intersect the layer containing  $s_i$ ; otherwise we call  $g$  *bad*.

Finally we briefly review the concept of bypassing introduced in [4] (see also Figure 12). We use here a version that is  $90^\circ$  rotated from the one in [4]. Recall that bends of a poly-line in  $\Gamma$  (like all bends and vertices of  $\Gamma$ ) are required to have integral  $y$ -coordinates.

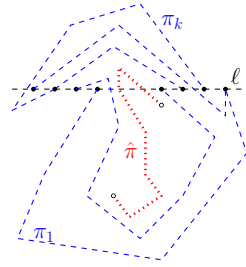


Figure 12: Poly-line  $\pi_1, \dots, \pi_k$  bypass poly-line  $\hat{\pi}$ .

**Definition 14** Let  $\pi_1, \dots, \pi_k$  be a set of poly-lines that are interior disjoint. Let  $\hat{\pi}$  be a poly-line that is disjoint from  $\pi_1, \dots, \pi_k$ . We say that  $\pi_1, \dots, \pi_k$  bypass  $\hat{\pi}$  if there exists a layer  $\ell$  such that

- layer  $\ell$  intersects  $\hat{\pi}$ ,
- for  $i = 1, \dots, k$ , the endpoints  $a_i, b_i$  of poly-line  $\pi_i$  are both in layer  $\ell$ , and
- for  $i = 1, \dots, k$ , any point in  $\hat{\pi} \cap \ell$  is between  $a_i$  and  $b_i$ .

**Lemma 7** [4] If a planar poly-line drawing  $\Gamma$  contains  $k$  poly-lines that bypass a poly-line  $\hat{\pi}$ , and if  $\hat{\pi}$  intersects  $h$  layers, then  $\Gamma$  uses at least  $h + k$  layers.

### 5.3 The ideal case

We first argue that  $h = h(w) + 5$  is impossible under some assumptions, and then show that this *ideal case* must occur somewhere in  $\Gamma$  (up to symmetry) if  $S$  and  $D$  are big enough. Formally, the ideal case occurs if the following conditions (C1-C4) hold (see also Figure 13):

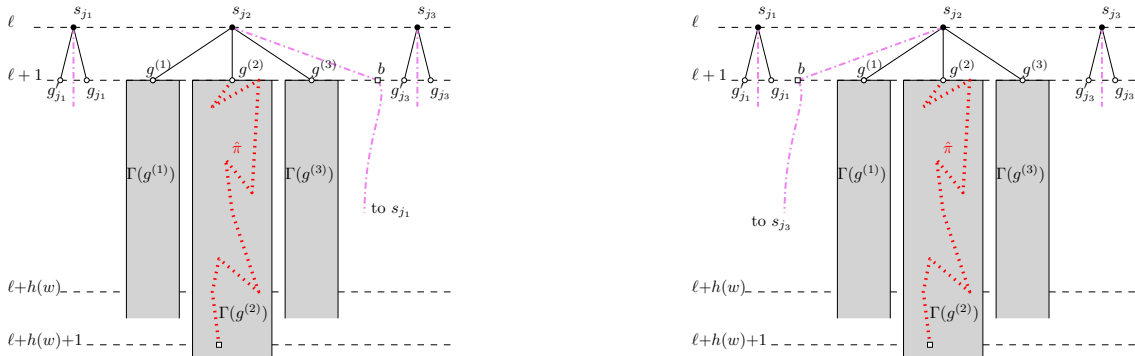


Figure 13: Illustration of the ideal case, both for  $g^{(3)} \prec b$  and  $b \prec g^{(1)}$ .

- (C1) There are three spine-vertices  $s_{j_1}, s_{j_2}, s_{j_3}$  that are all located in one layer  $\ell$  with  $\ell \leq \min\{5, h/2\}$ . Furthermore,  $1 \leq j_1 < j_2 < j_3 < S$  and  $s_{j_1} \prec s_{j_2} \prec s_{j_3}$ .

- (C2) For  $k = 1, 2, 3$ , vertex  $s_{j_k}$  has at least five good after-spine children that are on layer  $\ell + 1$ . Vertex  $s_{j_k}$  also has at least one before-spine child on layer  $\ell + 1$ .
- (C3) Among the five good after-spine children of  $s_{j_2}$  from (C2), there are three children  $g^{(1)}, g^{(2)}, g^{(3)}$  with  $g^{(1)} \prec g^{(2)} \prec g^{(3)}$  and age-order  $g^{(1)}, g^{(2)}, g^{(3)}$ .  
Furthermore, one of the spine-edges incident to  $s_{j_2}$  has a bend or endpoint  $b$  on layer  $\ell + 1$ . If  $b$  is on edge  $(s_{j_2}, s_{j_2-1})$  then  $g^{(3)} \prec b$ , otherwise  $b \prec g^{(1)}$ .
- (C4) There exists a path  $\hat{\pi}$  within  $\Gamma(g^{(2)})$  that intersects layer  $\ell+1$  and spans at least  $h(w) + 1$  layers. All points in  $\hat{\pi} \cap (\ell+1)$  are between  $g^{(1)}$  and  $g^{(3)}$ .

Assume for the rest of this subsection that (C1-C4) holds. For  $k = 1, 3$ , fix one before-spine child  $g'_{j_k}$  and one after-spine child  $g_{j_k}$  of  $s_{i_k}$  on layer  $\ell+1$ ; these exist by (C2). Now we define five interior-disjoint paths in  $H^-(C_{w+1})$  and the corresponding poly-lines  $\pi_1, \dots, \pi_5$  within  $\Gamma$  as follows (see also Figure 14):

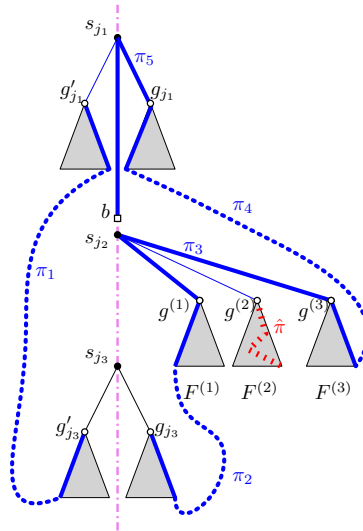


Figure 14: Five bypassing paths in  $H^-(C_{w+1})$ .

- $\pi_1$ : Follow the path that begins at  $g'_{j_1}$ , continues within  $F(g'_{j_1})$  to some leaf, and goes from there along cycle-edges to some leaf of  $F(g'_{j_3})$ . From there it goes upwards in the tree to  $g'_{j_3}$ . This poly-line uses only  $F(g'_{j_1})$  and  $F(g'_{j_3})$  and cycle-edges between them.
- $\pi_2$ : Follow the path that begins at  $g_{j_3}$ , continues within  $F(g_{j_3})$  to some leaf, and goes from there along cycle-edges to some leaf of  $F(g^{(1)})$ . From there it goes upwards in the tree to  $g^{(1)}$ . This poly-line uses only  $F(g_{j_3})$  and  $F(g^{(1)})$  and cycle-edges between them.
- $\pi_3$ : Follow the path  $\langle g^{(1)}, s_{j_2}, g^{(3)} \rangle$ , which uses only edges incident to  $s_{j_2}$ .
- $\pi_4$ : This poly-line is built symmetrically to  $\pi_2$ : begin at  $g_{j_1}$ , go to a leaf of  $F(g_{j_1})$ , from there along cycle-edges to a leaf of  $F(g^{(3)})$ , and from there to  $g^{(3)}$ . This poly-line uses only  $F(g_{j_1})$  and  $F(g^{(3)})$  and cycle-edges between them.

- $\pi_5$ : By (C3) some point  $b$  of a spine-edge incident to  $s_{j_2}$  lies on layer  $\ell + 1$ . Poly-line  $\pi_5$  begins at  $b$ , and goes along spine-edges, away from  $s_{j_2}$ , until it reaches either  $s_{j_1}$  or  $s_{j_3}$ . From there it goes to the after-spine child on layer  $\ell + 1$ , i.e., either  $g_{j_1}$  or  $g_{j_3}$ . Except for this last edge, poly-line  $\pi_5$  uses only spine-edges.

**Claim 15** *Poly-lines  $\pi_1, \dots, \pi_5$  bypass  $\hat{\pi}$ .*

**Proof:** Directly from the edges that they use, one observes that the five poly-lines  $\pi_1, \dots, \pi_5$  are disjoint from  $\hat{\pi}$ , and from each other except that they may have endpoints in common. (Here is it crucial that  $g^{(1)}$  is older than  $g^{(3)}$  so that the used cycle-edges are disjoint.) Assume that  $b$  belongs to  $(s_{j_2}, s_{j_2-1})$  (hence by (C3) we have  $g^{(3)} \prec b$ ), the other case is symmetric. Then all five poly-lines have one endpoint in  $\{g_{j_1}, g'_{j_1}, g^{(1)}\}$  and the other endpoint in  $\{g^{(3)}, b, g_{j_3}, g'_{j_3}\}$ . Observe that  $g_{j_1}$  is necessarily left of  $g^{(1)}$ , otherwise the straight-line segments  $(s_{j_1}, g_{j_1})$  and  $(s_{j_2}, g^{(1)})$  would intersect. Likewise  $g'_{j_1} \prec g^{(1)}$  and  $g^{(3)} \prec g_{j_3}, g'_{j_3}$ . So all five poly-lines connect a point on layer  $\ell + 1$  that is at or to the left of  $g^{(1)}$  with a point on layer  $\ell + 1$  that is at or to the right of  $g^{(3)}$ . Since  $\hat{\pi}$  uses only points on  $\ell + 1$  that are between  $g^{(1)}$  and  $g^{(3)}$  by (C4), the claim holds.  $\square$

Since  $\hat{\pi}$  spans  $h(w) + 1$  layers, therefore drawing  $\Gamma$  of  $H^-(C_{w+1})$  has at least  $(h(w) + 1) + 5$  layers, contradicting  $h = h(w) + 5$  as desired.

## 5.4 Existence of the ideal case

We now show that for  $S \geq 42$  and  $D \geq 81$ , conditions (C1-C4) hold. We note that these constants were chosen generously to keep the proof simpler; we can show (with lengthier arguments that we omit here) that  $S \geq 33$  and  $D \geq 21$  is sufficient, and likely even smaller constants would work.

### 5.4.1 Condition (C1)

Before arguing that (C1) holds, we first need various results about non-spine children of one fixed spine-vertex  $s_i$  with  $i < S$ .

**Observation 16** *For any non-spine child  $g$  of  $s_i$ ,  $\Gamma(g)$  intersects all layers in  $\{6, \dots, h(w)\}$ .*

**Proof:** There are  $h = h(w) + 5$  layers in total, and by induction  $\Gamma(g)$  intersects at least  $h(w)$  layers. Since  $F(g)$  is connected, therefore  $\Gamma(g)$  can avoid only the top five and the bottom five layers.  $\square$

**Claim 17** *At most 72 non-spine children of  $s_i$  are bad.*

**Proof:** We say that a non-spine child  $g$  has *type*  $(t, b)$  if the topmost and bottommost layer used by  $\Gamma(g)$  are  $t$  and  $b$ . By Observation 16 we have  $1 \leq t \leq 6$  and  $h(w) \leq b \leq h(w) + 5$ , so there are at most 36 types. Assume for contradiction that there are  $73 = 2 \cdot 36 + 1$  bad non-spine children of  $s_i$ , hence three of them (say  $g_1, g_2, g_3$ ) have the same type  $(t, b)$ .

Consider Figure 15. For  $k = 1, 2, 3$ , let  $B_k$  be a poly-line within  $\Gamma(g_k)$  that begins in layer  $t$  and ends in layer  $b$ . Let  $Q_k$  be a poly-line that starts at  $s_i$  (which is within layers  $\{t, \dots, b\}$  since  $g_k$  is bad), goes along the edge  $(s_i, g_k)$  (by Observation 13 this is a straight-line segment, hence also within  $\{t, \dots, b\}$ ) and continues within  $\Gamma(g_k)$  until it reaches  $B_k$ . Note that  $B_1 \cup Q_1$  and  $B_2 \cup Q_2$  and  $B_3 \cup Q_3$  are disjoint except at  $s_i$ , and reside entirely within layers  $\{t, \dots, b\}$ .

Exactly as in the proof of Lemma 5 in [1], one argues that this is impossible. Consider the drawing induced by  $\bigcup_k (B_k \cup Q_k)$ . Add a vertex  $v'$  in layer  $t - 1$  and connect it to the top ends of  $B_1, B_2, B_3$  (they are in layer  $t$ ). Likewise add a vertex  $v''$  in layer  $b + 1$  and connect it to the bottom ends of  $B_1, B_2, B_3$  (they are in layer  $b$ ). This gives a planar drawing of  $K_{3,3}$ , with  $\{s_i, v', v''\}$  as one side and the points  $B_k \cap Q_k$  for  $k = 1, 2, 3$  as the other side. Contradiction.  $\square$

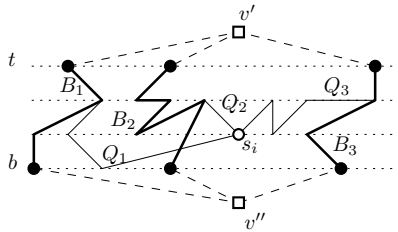


Figure 15: Three bad non-spine children of type  $(t, b)$  imply a planar drawing of  $K_{3,3}$ . (Picture based on [1]).

**Corollary 18** *The layer of  $s_i$  is in  $\{1, \dots, 5\} \cup \{h(w)+1, \dots, h(w)+5\}$ .*

**Proof:** If  $s_i$  were in any layer in  $\{6, \dots, h(w)\}$ , then by Observation 16 all  $2D > 72$  non-spine children of  $s_i$  would be bad, a contradiction to Claim 17.  $\square$

Now we explain how to satisfy (C1). By  $S \geq 42$  we have  $41 = 4 \cdot 10 + 1$  spine-vertices  $s_i$  for which  $i < S$ . Each of them is on one of 10 possible layers by Corollary 18. By the pigeon-hole principle, therefore at least five of these spine-vertices are on one layer  $\ell$ . After a possible vertical flip<sup>3</sup> of  $\Gamma$ , we may assume  $\ell \leq h/2$ . If  $w = 1$  then  $h = h(w) + 5 = 8$ , so  $\ell \leq 4$ . If  $w > 1$ , then  $h(w) > 3$  and therefore  $\ell \leq h/2 = \frac{1}{2}(h(w) + 5) < h(w) + 1$ ; by Corollary 18 therefore  $\ell \leq 5$ .

Among the five spine-vertices on  $\ell$ , we can (by the Erdős-Szekeres theorem [14]) find a subsequence of  $\lceil \sqrt{5} \rceil = 3$  spine-vertices  $s_{j_1}, s_{j_2}, s_{j_3}$  such that  $j_1 < j_2 < j_3$  and either  $s_{j_1} \prec s_{j_2} \prec s_{j_3}$  or  $s_{j_3} \prec s_{j_2} \prec s_{j_1}$ . After a possible horizontal flip<sup>3</sup> of  $\Gamma$  we have  $s_{j_1} \prec s_{j_2} \prec s_{j_3}$  and therefore (C1) holds.

### 5.4.2 From (C2) to (C3)

For the rest of the proof, we assume one particular choice of spine-vertices  $s_{j_1}, s_{j_2}, s_{j_3}$  satisfying (C1) has been fixed. We will defer the proof of condition (C2) to Subsection 5.4.4, since it will use some more complicated ingredients. Instead we show here that (C2) implies (C3). We first need a few more observations about non-spine children.

**Observation 19** *Assume that  $s_{j_k}$  (for some  $k \in \{1, 2, 3\}$ ) has  $t \geq 3$  non-spine children  $g_1, \dots, g_t$  in layer  $\ell + 1$ , with  $g_1 \prec \dots \prec g_t$ . Then the ccw order of neighbours at  $s_{j_k}$  contains  $g_1, \dots, g_t$  as subsequence.*

**Proof:** By Observation 13 edge  $(s_{j_k}, g_i)$  is a straight-line segment for all  $i = 1, \dots, t$ . Since the drawing is plane and  $g_1, \dots, g_t$  are all on the layer below  $s_{j_k}$ , the order of  $g_1, \dots, g_t$  on the layer must reflect the ccw order at  $s_{j_k}$ .  $\square$

<sup>3</sup>Note that flipping the drawing reverses all edge-orders, so we might be proving a lower bound for  $C_{w+1}^{\text{rev}}$ . But  $C_{w+1}^{\text{rev}}$  is isomorphic to  $C_{w+1}$ , so their skirted graphs are isomorphic and this is not a problem.

**Observation 20** Assume that  $s_{j_k}$  (for some  $k \in \{1, 2, 3\}$ ) has after-spine children  $g_1, \dots, g_5$  in layer  $\ell+1$ , with  $g_1 \prec \dots \prec g_5$ . Then  $g_1, g_2, g_3$  or  $g_3, g_4, g_5$  (or both) are in age-order.

**Proof:** Let  $g_y$  (with  $1 \leq y \leq 5$ ) be the youngest among children  $g_1, \dots, g_5$ . Since  $g_1, \dots, g_5$  reflect the ccw order of neighbours at  $s_{j_k}$  by Observation 19, the age-order among  $g_1, \dots, g_5$  hence is  $g_{y+1}, \dots, g_5, g_1, \dots, g_y$ . If  $y \geq 3$  then  $g_1, g_2, g_3$  are hence in age-order, otherwise  $y \leq 2$  and  $g_3, g_4, g_5$  are in age-order.  $\square$

Now assume that (C2) holds, and let  $g_1, \dots, g_5$  be the five good after-spine children of  $s_{j_2}$  on layer  $\ell+1$ , in left-to-right order. We can find the subsequence  $g^{(1)}, g^{(2)}, g^{(3)}$  in age-order from Observation 20. To find point  $b$ , let  $g'$  be the before-spine child of  $s_{j_k}$  on layer  $\ell+1$  that exists by (C2).

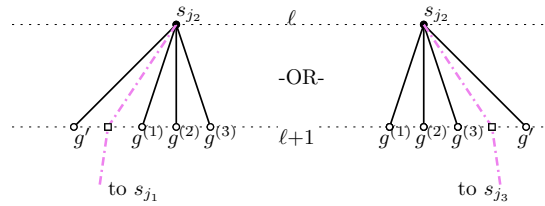


Figure 16: Possible arrangements of non-spine children of  $s_{j_2}$  on layer  $\ell + 1$ .

Consider Figure 16. If  $g' \prec g^{(1)}$ , then to reflect the ccw order at  $s_{j_2}$ , the spine-edge  $(s_{j_2}, s_{j_2+1})$  (which lies in ccw order between  $g'$  and  $g^{(1)}$ ) has a bend or endpoint  $b$  on layer  $\ell + 1$ , and  $g' \prec b \prec g^{(1)}$ . This satisfies all conditions of (C3). Similarly if  $g^{(3)} \prec g'$  then spine-edge  $(s_{j_2}, s_{j_2-1})$  has a bend or endpoint on layer  $\ell + 1$  and (C3) holds. Finally  $g^{(1)} \prec g' \prec g^{(3)}$  is impossible since this would violate the ccw order at  $s_{i_k}$  due to Observation 19 and since  $g^{(3)}$  is younger than  $g^{(1)}$ . So (C2) implies (C3).

### 5.4.3 From (C3) to (C4)

Now we show that (C3) implies (C4), but we phrase this claim more generally since we need it also to argue (C2) below.

**Claim 21** Assume  $s_{j_k}$  (for  $k \in \{1, 2, 3\}$ ) has three good after-spine children  $g^{(1)}, g^{(2)}, g^{(3)}$  on layer  $\ell + 1$  with  $g^{(1)} \prec g^{(2)} \prec g^{(3)}$  and age-order  $g^{(1)}, g^{(2)}, g^{(3)}$ . Then there exists a path  $\hat{\pi}$  within  $\Gamma(g^{(2)})$  that intersects layers  $\ell+1, \dots, \ell+h(w)+1$ , and all points in  $\hat{\pi} \cap (\ell + 1)$  are between  $g^{(1)}$  and  $g^{(3)}$ .

**Proof:** Figure 17 illustrates the setup for this claim. Let  $\mathcal{I}$  be the closed interval of points on layer  $\ell + 1$  between  $g^{(1)}$  and  $g^{(3)}$ , so the path  $\hat{\pi}$  that we want to find should intersect layer  $\ell + 1$  only in  $\mathcal{I}$ . Recall that  $F(g^{(2)})$  denotes the copy of  $F_w$  attached at  $g^{(2)}$ , and that  $g^{(2)}$  has a child  $p$  and a grand-child  $r$  that is a root of a copy of  $C_w$ . We use the notation  $C$  for this copy of  $C_w$ . We need an observation.

**Observation 22**  $H^-(C)$  uses no points in  $\mathcal{I}$ .

**Proof:** Define a cycle  $\kappa$  as follows (see also Figure 17a). Start at child  $p$  of  $g^{(2)}$ , go to its last child (which is a leaf of  $F(g^{(2)})$ ) and go from there along the cycle-edges to a leaf of  $F(g^{(3)})$ . Go upwards in tree  $F(g^{(3)})$  to  $g^{(3)}$  and from there to  $s_{j_k}$ . Continue symmetrically through  $F^{(1)}$ , i.e.,

go from  $s_{j_k}$  to  $g^{(1)}$  to a leaf of  $F(g^{(1)})$ , then along cycle-edges to the first child of  $p$  and then to  $p$ . Cycle  $\kappa$  has  $g^{(2)}$  and  $r$  on opposite sides due to the ccw order at  $p$ .

Now study the closed poly-line  $K$  traced by  $\kappa$  in  $\Gamma$ . Since  $\langle g^{(1)}, s_i, g^{(3)} \rangle$  is drawn with straight-line segments between layers  $\ell + 1$  and  $\ell$ , all points of  $\mathcal{I}$  are on the same side of  $K$  as  $g^{(2)}$  (or on  $K$ ). Since  $r$  (and therefore all of  $H^-(C)$ ) is on the opposite side of  $\kappa$  in the plane drawing, the claim holds.  $\square$

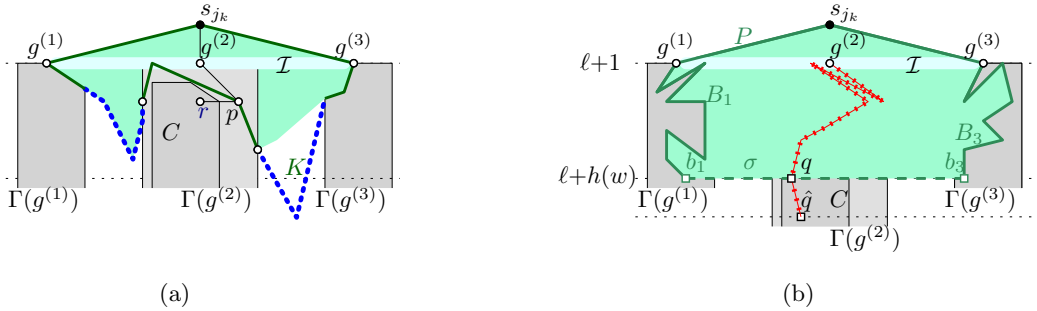


Figure 17: (a) Poly-line  $K$  separates  $\mathcal{I}$  from  $H^-(C)$ . (b) The pocket  $P$ .

Let the *pocket*  $P$  be defined as follows, see also Figure 17b. For  $k = 1, 3$ , child  $g^{(k)}$  is good, hence  $\Gamma(g^{(k)})$  contains no point of layer  $\ell$ , and hence contains points in layers  $\ell+1, \dots, \ell + h(w)$  (and possible other layers below). Let  $B_k$  be a poly-line within  $\Gamma(g^{(k)})$  that connects  $g^{(k)}$  to a point  $b_k$  on layer  $\ell + h(w)$ . Choose  $b_k$  such that  $B_k$  is minimal, i.e., no subset of  $B_k$  would do; in particular all points in  $B_k \setminus b_k$  are above layer  $\ell+h(w)$ . This implies that  $b_1 \prec b_3$  since  $g^{(1)} \prec g^{(3)}$  and poly-lines  $B_1$  and  $B_3$  are disjoint and intersect the same set of layers. Let the *lid*  $\sigma$  be the line-segment  $\overline{b_1 b_3}$ ; note that  $\sigma$  is not necessarily a segment of  $\Gamma$ . Now define pocket  $P$  to be the closed set bounded by  $B_1 \cup \langle g^{(1)}, s_i, g^{(3)} \rangle \cup B_3 \cup \sigma$ .

Note that the points that belong both to layer  $\ell+1$  and to the interior of  $P$  belong to  $\mathcal{I}$ , because  $B_1$  and  $B_3$  are in layer  $\ell+1$  and below. Assume for contradiction that all of  $\Gamma(g^{(2)})$  (and in particular therefore  $H^-(C)$ ) resides within pocket  $P$ . Since  $\Gamma(g^{(2)})$  is disjoint from  $\Gamma(g^{(1)})$ ,  $\Gamma(g^{(3)})$  and poly-line  $\langle g^{(1)}, s_{j_k}, g^{(2)} \rangle$ , it resides in the interior of  $P$ , except perhaps at lid  $\sigma$ . Therefore any points of  $\Gamma(g^{(2)})$  on layer  $\ell + 1$  are in the interior of  $P$ , hence in  $\mathcal{I}$ . But  $H^-(C) \subset \Gamma(g^{(2)})$  uses no points on layer  $\ell + 1$  by Observation 22. Therefore  $H^-(C)$  contains no points on layer  $\ell + 1$ , hence fits within  $h(w) - 1$  layers, a contradiction.

So  $\Gamma(g^{(2)})$  must use points outside  $P$ , and also inside  $P$  (at  $g^{(2)}$ ), and by connectivity hence contains points on the boundary of  $P$ . As discussed above, therefore  $\Gamma(g^{(2)})$  contains a point  $q$  on the interior of lid  $\sigma$ . Furthermore, to reach the outside of  $P$  there must (for some choice of  $q$ ) be a poly-line within  $\Gamma(g^{(2)})$  that goes downward from  $q$ . Let  $\hat{q}$  be the next bend of this edge, which is on layer  $\ell + h(w) + 1$  by the preprocessing. Let  $\hat{\pi}$  be the poly-line within  $\Gamma(g^{(2)})$  from  $g^{(2)}$  (on layer  $\ell + 1$ ) to point  $\hat{q}$  (on layer  $\ell + h(w) + 1$ ). If we choose  $q$  such that  $\hat{\pi}$  is minimal, then with the exception of the segment from  $q$  to  $\hat{q}$ , poly-line  $\hat{\pi}$  is inside pocket  $P$ . In particular  $\hat{\pi}$  uses no points on layer  $\ell + 1$  except the ones that are in the pocket, hence on  $\mathcal{I}$ . This proves the claim.  $\square$

Applying Claim 21 to the three vertices  $g^{(1)}, g^{(2)}, g^{(3)}$  from Condition (C3) shows that (C3) implies (C4).

### 5.4.4 Condition (C2)

With Claim 21 in hand, we are finally in a position to prove that Condition (C2) holds. Consider vertex  $s_{j_k}$  (for  $k \in \{1, 2, 3\}$ ), which we know by (C1) to be on layer  $\ell$  with  $\ell \leq \min\{5, h/2\}$ . Vertex  $s_{j_k}$  has at least  $D - 72 \geq 9$  good after-spine children by Claim 17. Any such good child  $g$  cannot be on layer  $\ell$  by definition of good, so  $g$  is on layer  $\ell - 1$  or  $\ell + 1$  by Observation 13.

Assume for contradiction that there are at most four good after-spine children on layer  $\ell + 1$ . So there are (at least) five good after-spine children that are on layer  $\ell - 1$ ; enumerate them as  $g_1, \dots, g_5$  with  $g_1 \prec \dots \prec g_5$ . Drawing  $\Gamma(g_i)$  (for  $i = 1, \dots, 5$ ) cannot use layer  $\ell$  since  $g_i$  is good, and uses layer  $\ell - 1$  at  $g_i$ , so it must fit within layers  $1, \dots, \ell - 1$ . This implies  $\ell > h(w)$  since  $\Gamma(g_i)$  uses at least  $h(w)$  layers by induction.

If  $w \geq 2$  then this is impossible, because then  $h(w) \geq 9$  while  $\ell \leq 5$  by (C1). So we must have  $w = 1$ , hence  $h(w) = 3$ , and we know  $\ell > 3$ . But we also know that  $h = h(w) + 5 = 8$  and  $\ell \leq h/2 = 4$ , so  $\ell = 4$ . For purposes of applying Claim 21, rotate  $\Gamma$  by  $180^\circ$  to obtain drawing  $\Gamma'$ . Since  $\Gamma$  has 8 layers,  $s_i$  (which was on layer  $\ell = 4$  in  $\Gamma$ ) is located on layer 5 in  $\Gamma'$ . Furthermore, its after-spine children  $g_5, \dots, g_1$  are on layer 6 (in this order), and their drawings only use layers 6, 7, 8. By Observation 20, either  $g_5, g_4, g_3$  or  $g_3, g_2, g_1$  are in age-order. By Claim 21 drawing  $\Gamma'(g_2)$  or  $\Gamma'(g_4)$  contain a path  $\hat{\pi}$  that spans  $h(w) + 1 = 4$  layers. Contradiction, so (in  $\Gamma$ ) there are at least five good after-spine children of  $s_{j_k}$  on layer  $\ell + 1$ . This proves the claim of (C2) about after-spine children, and the claim about before-spine children is proved similarly.

So we know (C1) and (C2) hold if  $S \geq 42$  and  $D \geq 81$ , and we have argued that (C2) implies (C3) which in turn implies (C4). This proves Lemma 6.

## 5.5 Proving the lower bounds

With Lemma 6 in place, we can now prove the lower-bound theorems. To do so, we first bound the (rooted) pathwidth of  $F_w$  and trees derived from it.

**Observation 23** *We have  $rpw(F_w) \leq w + 1$ , and for  $w \geq 2$  one possible spine for the rooted pathwidth is  $\langle g, p, s_1, \dots, s_S \rangle$ .*

*Let  $F_w''$  be the leaf-reduction of the inner skeleton of  $H(F_w)$ . Then  $pw(F_w'') \leq w - 1$ , and for  $w \geq 2$  one possible main path for the pathwidth ends at the root.*

**Proof:** We proceed by induction on  $w$ . Tree  $F_1$  consists of a path  $\langle g, p, r, c \rangle$  with leaves attached; this has rooted pathwidth 2. Also  $F_1''$  is a single vertex, since it is obtained from  $F_1$  by first deleting all leaves (this gives a path), and then doing the leaf-reduction. So  $pw(F_1'') = 0$ .

Now consider  $F_{w+1}$  for  $w \geq 1$ . This consists of a path  $\langle g, p, s_1, \dots, s_S \rangle$  with some leaves and some copies of  $F_w$  attached. Using this path as spine, we immediately get  $rpw(F_{w+1}) \leq rpw(F_w) + 1 \leq w + 2$ . Also,  $F_{w+1}''$  consists of path  $\langle g, p, s_1, \dots, s_{S-1} \rangle$  with copies of  $F_w''$  attached; using this path as main path therefore  $pw(F_{w+1}'') \leq pw(F_w'') + 1 \leq w$ . □

Thus far all constructions and lower bounds have been for plane drawings. But we can easily prove lower bounds even if only planarity is required.

**Proof: (of Theorem 9)** We want to construct a regular Halin-graph  $H(T)$  such that any planar poly-line drawing of  $H(T)$  requires at least  $6pw(T'') + 3$  layers, where  $T''$  is the leaf-reduction of the inner skeleton of  $H(T)$ .

For any  $w \geq 2$ , consider the tree  $T$  obtained by taking two copies of  $F_w$  and combining them by adding an edge between the two copies of the root  $g$ . Then  $T$  has no vertex of degree 2, so  $H(T)$

is regular. Fix an arbitrary planar poly-line drawing  $\Gamma$  of  $H(T)$ . Since  $H(T)$  is 3-connected [22], drawing  $\Gamma$  either respects the ccw orders at all vertices, or it uses the reverse orders everywhere (in case of which we flip  $\Gamma$  horizontally and then it respect the ccw orders). But it is possible that the infinite region of  $\Gamma$  is incident to some *inner face* of  $H(T)$ , i.e., some face different from the one bounded by the cycle-edges. Tree  $T$  contains two copies of  $F_w$ , and the infinite region of  $\Gamma$  can be an inner face of  $H^-(F_w)$  for at most one of them. Therefore  $\Gamma$  contains a plane drawing of  $H^-(F_w)$ , hence also one of  $H^-(C_w)$ . By Lemma 6 this requires at least  $h(w) = 6w - 3$  layers.

Now consider the leaf-reduction  $T''$  of the inner skeleton of  $T$ . For  $w = 1$ , the inner skeleton is a path and hence  $T''$  is a single vertex with pathwidth  $0 = w - 1$ . For  $w \geq 2$ , the leaf-reduction  $T''$  consists of two copies of  $F''_w$  (defined as in Observation 23). Each copy has pathwidth at most  $w - 1$ , and this bound is obtained with a main path that ends at the root. Therefore we can combine these two paths into one path and use it as main path for  $T''$  to show  $pw(T'') \leq w - 1$ . Thus  $H(T)$  requires  $6w - 3 \geq 6pw(T'') + 3$  layers.  $\square$

We note that this lower bound implies a lower bound of  $\Omega(\log n)$  on the height, since  $C_w$  contains  $c^w$  vertices for some (rather large) constant  $c$ . However, this is not a new result; any Halin-graph where the skeleton contains a tree of pathwidth  $\Omega(\log n)$  (e.g. a complete binary tree) requires height  $\Omega(\log n)$  [15]. The main contribution of Theorem 9 is that it matches the upper bound in Theorem 1. (This was also the reason why we used the leaf-reduction of the inner skeleton, rather than the skeleton, in Theorem 1.)

**Proof: (of Theorem 10)** We want to construct a regular Halin-graph  $H(T)$  such that any planar poly-line drawing of  $H(T)$  requires at least  $6rpw_{\min}(T) - 9$  layers.

For any  $w \geq 2$ , again let  $T$  be two copies of  $F_w$ , combined by adding an edge between the two copies of  $g$ . We know that  $rpw(F_w) \leq w + 1$ . The spine of  $F_w$  is  $\langle g, p, s_1, \dots, s_S \rangle$ ; if we root  $T$  at one copy of  $s_S$  then we can use as its spine the two combined spines of the two copies of  $F_w$  and so have  $rpw_{\min}(T) = rpw(F_w) \leq w + 1$ . Graph  $H(T)$  is a regular Halin-graph and since (as above) any planar drawing of it includes a plane drawing of  $H^-(C_w)$ , graph  $H(T)$  requires at least  $h(w) = 6w - 3 \geq 6rpw_{\min}(T) - 9$  layers by Lemma 6.  $\square$

**Proof: (of Theorem 11)** We want to show that there exists an extended Halin-graph  $H(T)$  such that any planar poly-line drawing of  $H(T)$  requires at least  $6rpw(T) - 7$  layers. We give the lower bound only for a plane poly-line drawing; it can be converted to one for planar poly-line drawings by doubling the tree as above.

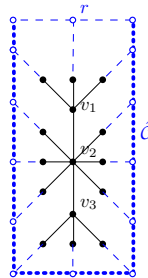


Figure 18: The modified construction for Theorem 11. Tree  $T_1$  uses black circles.

We construct a rooted tree  $\hat{C}_w$  that differs from  $C_w$  only in the base case. See Figure 18. Start with the tree  $T_1$  from [1] that requires 3 layers in any plane drawing. This tree consists of a path

$\langle v_1, v_2, v_3 \rangle$ , with three leaves attached at each of  $v_1, v_3$ , and six leaves attached at  $v_2$ , three on each side of path  $\langle v_1, v_2, v_3 \rangle$ . To obtain  $\hat{C}_2$ , attach a degree-1 vertex at every degree-1 vertex of  $T_1$ , and let  $r$  be the middle of the new degree-1 vertices near  $v_1$ . Make  $r$  the root, and add two further children at  $r$  that become first and last leaf of the resulting tree  $\hat{C}_2$ . Note that  $H^-(\hat{C}_2)$  consists of a cycle  $\hat{C}$  (using the cycle-edges and edges from  $r$  to the first and last leaf) that surrounds  $T_1$ . Any plane poly-line drawing of  $H^-(\hat{C}_2)$  therefore requires five layers because  $\hat{C}$  encloses the drawing of  $T_1$  that requires 3 layers. Also note that  $rpw(\hat{C}_2) = 2$ , using the path from  $r$  to  $v_3$  as the spine.

Now construct  $\hat{F}_w$  from  $\hat{C}_w$  and  $\hat{C}_{w+1}$  from  $\hat{F}_w$  exactly as done in Definition 12. Set  $\hat{h}(2) = 5$  and  $\hat{h}(w) = \hat{h}(w-1) + 6$  for  $w \geq 3$ . Then  $H^-(\hat{C}_w)$  requires  $\hat{h}(w)$  layers in any plane poly-line drawing, because this was shown for  $\hat{C}_2$  above, and is proved for  $\hat{C}_w$  for  $w \geq 3$  exactly as the induction step of Lemma 6. Also as before  $rpw(\hat{C}_w) \leq rpw(\hat{C}_{w-1}) + 1$  for  $w \geq 3$ , therefore  $rpw(\hat{C}_w) \leq w$ . So any plane drawing of  $H(\hat{C}_w)$  (which includes  $H^-(\hat{C}_w)$ ) must use  $\hat{h}(w) = 6w - 7 \geq 6rpw(\hat{C}_w) - 7$  layers.  $\square$

## 6 Conclusion

In this paper, we studied drawings of Halin-graphs whose height depends on the pathwidth of the skeleton and therefore is within a constant factor of the optimum height. We gave a 6-approximation for the height of poly-line drawings of such graphs, and a 12-approximation for the height of straight-line drawings. We also showed that there exists a Halin-graph for which our constructions give the minimum possible height. Many open problems remain:

- Can we find straight-line drawings of height  $c \cdot pw(T) + O(1)$ , for  $c < 12$  and ideally  $c = 6$ ?
- We have focused on the height and ignored the width. For straight-line drawings, the detour through flat visibility representations means that the width may be exponential [3]. Are there straight-line drawings of height  $O(pw(T))$  for which the width is polynomial (and preferably linear)?

Last but not least, are there other planar graph classes that have approximation algorithms for height (or perhaps the area) of planar graph drawings?

## References

- [1] J. Batzill and T. Biedl. Order-preserving drawings of trees with approximately optimal height (and small width). *Journal of Graph Algorithms and Applications*, 24(1):1–19, 2020. doi:10.7155/jgaa.00515.
- [2] T. Biedl. Small drawings of outerplanar graphs, series-parallel graphs, and other planar graphs. *Discrete and Computational Geometry*, 45(1):141–160, 2011. doi:10.1007/s00454-010-9310-z.
- [3] T. Biedl. Height-preserving transformations of planar graph drawings. In C. Duncan and A. Symvonis, editors, *Graph Drawing (GD'14)*, volume 8871 of *Lecture Notes in Computer Science*, pages 380–391. Springer, 2014. doi:10.1007/978-3-662-45803-7\_32.
- [4] T. Biedl. Optimum-width upward drawings of trees. Technical report, ArXiv, 2015. CoRR 1506.02096.

- [5] T. Biedl. Horton-Strahler number, rooted pathwidth and minimum-width upward drawings of trees. *Information Processing Letters*, 175:106230, 2022. doi:10.1016/j.ipl.2021.106230.
- [6] T. Chan. Tree drawings revisited. *Discrete and Computational Geometry*, 63(4):799–820, 2020. doi:10.1007/s00454-019-00106-w.
- [7] P. Crescenzi, G. Di Battista, , and A. Piperno. A note on optimal area algorithms for upward drawings of binary trees. *Computational Geometry: Theory and Applications*, 2:187–200, 1992. doi:10.1016/0925-7721(92)90021-J.
- [8] P. Crescenzi, P. Penna, , and A. Piperno. Linear area upward drawings of AVL trees. *Computational Geometry: Theory and Applications*, 9(1-2):25–42, 1998. doi:10.1016/S0925-7721(97)00013-8.
- [9] H. de Fraysseix, J. Pach, , and R. Pollack. Small sets supporting Fary embeddings of planar graphs. In *ACM Symposium on Theory of Computing (STOC '88)*, pages 426–433, 1988. doi:10.1145/62212.62254.
- [10] H. de Fraysseix, J. Pach, , and R. Pollack. How to draw a planar graph on a grid. *Combinatorica*, 10:41–51, 1990. doi:10.1007/BF02122694.
- [11] R. Diestel. *Graph Theory, 4th Edition*, volume 173 of *Graduate texts in mathematics*. Springer, 2012.
- [12] P. Eades, Q. Feng, X. Lin, , and H. Nagamochi. Straight-line drawing algorithms for hierarchical graphs and clustered graphs. *Algorithmica*, 44(1):1–32, 2006. doi:10.1007/s00453-004-1144-8.
- [13] D. Eppstein. Simple recognition of Halin graphs and their generalizations. *Journal of Graph Algorithms and Applications*, 20(2):323–346, 2016. doi:10.7155/jgaa.00395.
- [14] P. Erdős and G. Szekeres. A combinatorial problem in geometry. *Compositio Mathematica*, 2, 1935.
- [15] S. Felsner, G. Liotta, , and S. Wismath. Straight-line drawings on restricted integer grids in two and three dimensions. *Journal of Graph Algorithms and Applications*, 7(4):335–362, 2003. doi:10.7155/jgaa.00075.
- [16] F. Fomin and D. Thilikos. A 3-approximation for the pathwidth of Halin graphs. *Journal of Discrete Algorithms*, 4(4):499–510, 2006. doi:10.1016/j.jda.2005.06.004.
- [17] M. Francis and A. Lahiri. VPG and EPG bend-numbers of Halin graphs. *Discrete Applied Mathematics*, 215:95–105, 2016. doi:10.1016/j.dam.2016.07.007.
- [18] F. Frati. Straight-line drawings of outerplanar graphs in  $O(dn \log n)$  area. *Computational Geometry: Theory and Applications*, 45(9):524–533, 2012. doi:10.1016/j.comgeo.2010.03.007.
- [19] F. Frati, M. Patrignani, , and V. Roselli. LR-drawings of ordered rooted binary trees and near-linear area drawings of outerplanar graphs. *Journal of Computers and System Sciences*, 107:28–53, 2020. doi:10.1016/j.jcss.2019.08.001.

- [20] A. Garg, M.T. Goodrich, , and R. Tamassia. Planar upward tree drawings with optimal area. *International Journal of Computational Geometry and Applications*, 6:333–356, 1996. doi:10.1142/S0218195996000228.
- [21] A. Garg and A. Rusu. Area-efficient order-preserving planar straight-line drawings of ordered trees. *International Journal of Computational Geometry and Applications*, 13(6):487–505, 2003. doi:10.1142/S021819590300130X.
- [22] R. Halin. Studies on minimally  $n$ -connected graphs. In *Combinatorial Mathematics and its Applications (Proc. Conf., Oxford, 1969)*, pages 129–136. Academic Press, 1971.
- [23] J. Pach and G. Tóth. Monotone drawings of planar graphs. *Journal of Graph Theory*, 46(1):39–47, 2004. doi:10.1002/jgt.10168.
- [24] P. Scheffler. A linear-time algorithm for the pathwidth of trees. In R. Bodendieck and R. Henn, editors, *Topics in Combinatorics and Graph Theory*, pages 613–620. Physica-Verlag Heidelberg, 1990.
- [25] W. Schnyder. Embedding planar graphs on the grid. In *ACM-SIAM Symposium on Discrete Algorithms (SODA '90)*, pages 138–148, 1990.
- [26] M. Skowronska and M. Syslo. Dominating cycles in Halin graphs. *Discrete Mathematics*, 86(1-3):215–224, 1990. doi:10.1016/0012-365X(90)90362-L.
- [27] M. Suderman. Pathwidth and layered drawings of trees. *International Journal of Computational Geometry and Applications*, 14(3):203–225, 2004. doi:10.1142/S0218195904001433.
- [28] M. Syslo and A. Proskurowski. On Halin graphs. In *Graph Theory*, volume 1018 of *Lecture Notes in Mathematics*, pages 248–256. Springer, 1983. doi:10.1007/BFb0071635.